

Dimensional reduction in anomaly mediation

Ed Boyda

Department of Physics, University of California, Berkeley, California 94720

Hitoshi Murayama and Aaron Pierce

*Department of Physics, University of California, Berkeley, California 94720**and Theory Group, Lawrence Berkeley National Laboratory, Berkeley, California 94720*

(Received 28 September 2001; published 8 April 2002)

We offer a guide to dimensional reduction in theories with anomaly-mediated supersymmetry breaking. Evanescent operators proportional to ϵ arise in the bare Lagrangian when it is reduced from $d=4$ to $d=4-2\epsilon$ dimensions. In the course of a detailed diagrammatic calculation, we show that inclusion of these operators is crucial. The evanescent operators conspire to drive the supersymmetry-breaking parameters along anomaly-mediation trajectories across heavy particle thresholds, guaranteeing the ultraviolet insensitivity.

DOI: 10.1103/PhysRevD.65.085028

PACS number(s): 12.60.Jv

I. INTRODUCTION

Anomaly mediation is a remarkably predictive framework for supersymmetry breaking in which the breaking of scale invariance mediates between hidden and visible sectors [1,2]. Since the soft supersymmetry-breaking parameters are determined by the breaking of scale invariance, they can be written in terms of beta functions and anomalous dimensions in relations which hold at all energies. An immediate consequence is that supersymmetry-breaking terms are completely insensitive to physics in the ultraviolet. Anomalous dimensions and beta functions, which depend only on degrees of freedom excitable at a given energy, completely specify the soft parameters at that energy. This property makes anomaly mediation an attractive solution to the supersymmetric flavor problem. The low-energy spectrum of soft masses and couplings is independent of the physics that explains flavor in the ultraviolet.¹

On the other hand, regularization by dimensional reduction (DRED) [6] is often the preferred regulator for supersymmetric field theories. As with ordinary dimensional regularization (DREG), DRED is simpler computationally than Pauli-Villars or other cutoff methods. DRED is also superior to DREG in that it preserves supersymmetry: In DREG when we analytically continue the dimension of space-time away from $d=4$, the spinor algebra changes, creating a mismatch between fermionic and bosonic degrees of freedom. DRED avoids this problem by compactifying from $d=4$ to $d=4-2\epsilon$ dimensions and making the fields independent of the extra 2ϵ dimensions. The spinor algebra does not change, so the regulated theory is still supersymmetric.

In this paper we explore the subtleties of DRED in theories with anomaly-mediated supersymmetry breaking. We point out that it is not correct to just add anomaly-mediated

supersymmetry breaking to the Lagrangian if DRED is used. Since most calculations in the literature are done this way, our result raises a warning flag. In retrospect, it is not surprising why it is so. In the case of the chiral anomaly, one does not add the chiral anomaly as an additional term to the Lagrangian. When the theory is properly regularized, the chiral anomaly is the outcome rather than a part of the input Lagrangian. Similarly, the anomaly-mediated supersymmetry breaking must be the outcome of the Lagrangian rather than the additional terms in the bare Lagrangian. We show that the most important consequence of compactifying to $4-2\epsilon$ dimensions is the introduction of evanescent operators, proportional to ϵ , into the bare Lagrangian. These operators prove to be of first importance in diagrammatic anomaly-mediation calculations. Proper inclusion of these operators yields a DRED-based formalism suitable for anomaly-mediation calculations. In addition we discuss the implications of DRED's failure to regulate infrared divergences, which follows because the dimension of space-time is necessarily $d < 4$ in DRED.

As a showcase for our DRED-based anomaly mediation formalism, we perform an explicit diagrammatic calculation that shows the ultraviolet insensitivity of anomaly mediation. Although the appearance of supersymmetry-breaking parameters and the decoupling of flavor physics have been well understood through the spurion formalism (see [3] for the most comprehensive review of anomaly mediation using the spurion formalism), the phenomena have not been investigated in a diagrammatic framework. The spurion analysis fixes the A terms to be

$$A_{ijk} = -m_{3/2} \lambda_{ijk} (\gamma_i + \gamma_j + \gamma_k), \quad (1.1)$$

while scalar masses are given by

$$\tilde{m}_i^2 = \frac{1}{2} |m_{3/2}|^2 \dot{\gamma}_i. \quad (1.2)$$

Here, $m_{3/2}$ is the gravitino mass, λ_{ijk} is the superpotential Yukawa coupling, $\gamma_i \equiv -\frac{1}{2} \mu (d/d\mu) \log Z_i$ is the anomalous

¹This property has led to the well known issue of tachyonic sleptons. People have taken various approaches towards solving this problem [1,3,4] which jeopardize the ultraviolet insensitivity. However, it was shown recently that the UV insensitivity can be preserved while solving the problem of tachyonic sleptons [5].

dimension of the i th superfield, and $\dot{\gamma}_i \equiv \mu(d/d\mu)\gamma_i$. To fix signs, these terms appear in the Lagrangian as

$$\mathcal{L} \ni -\tilde{m}_i^2 \tilde{Q}_i^* \tilde{Q}_i - A_{ijk} \tilde{Q}_i \tilde{Q}_j \tilde{Q}_k + \text{H.c.}, \quad (1.3)$$

with scalar fields \tilde{Q}_i . It is highly non-trivial that the forms in Eqs. (1.1) and (1.2) indeed are invariant under the renormalization-group evolution, which was checked explicitly in [7]. We apply our DRED calculation to see in detail how various diagrams conspire to set the soft parameters on their anomaly-mediated trajectories across the massive particle thresholds. In particular, loops containing evanescent ϵ operators produce the soft terms above the threshold of flavor physics, and additional evanescent operators combine with the flavor fields to decouple the flavor sector below threshold. We find that when calculating with DRED, it is inconsistent to simply insert the soft terms of Eqs. (1.1) and (1.2) into the Lagrangian while neglecting the evanescent operators.

In Sec. II we review some established results of anomaly-mediated supersymmetry breaking. In Sec. III we present a puzzle that makes clear the need to develop a consistent framework for using DRED with anomaly mediation. In Sec. IV we focus on developing this framework, deriving the dimensionally reduced bare Lagrangian. In Sec. V, we utilize this Lagrangian to discuss the origin of Eqs. (1.1) and (1.2). Having established a framework for using DRED with anomaly mediation, we demonstrate its use through explicit diagrammatic calculations which confirm the UV insensitivity of anomaly mediation. In Sec. VI we take a moment to recapitulate, and emphasize the basic message of our derivation of the anomaly-mediated DRED-based formalism. Section VII defines the models used in our diagrammatic calculations. In Sec. VIII we compute the A terms, a short one-loop calculation. In Sec. IX we discuss the substantially more complicated case of the scalar masses, which is a two-loop calculation.

II. ANOMALY MEDIATION AND HOLOMORPHIC REGULARIZATION

In this section we provide a brief review of established results in anomaly-mediated supersymmetry breaking. We discuss the origin of the anomaly-mediated contributions. We also review the spurion analysis for regularization schemes that use an explicit cutoff. This discussion will provide a useful foil for the DRED scheme which we later employ.

In anomaly-mediated models of supersymmetry breaking [1,2], the sole source of supersymmetry breaking resides in the chiral compensator field in the supergravity Lagrangian: $\langle \Phi \rangle = 1 + m_{3/2} \theta^2$. We now review the origin of this field. Supergravity is not scale invariant because it has an explicit mass scale: the Planck scale. However, it is possible to reformulate the theory as conformal supergravity by compensating for the non-invariance of the Lagrangian under super-Weyl transformations by a fictitious transformation of the chiral compensator field Φ .

The supersymmetry (SUSY) breaking that arises when the chiral compensator takes on its vacuum expectation value

will always be present. However, in general, M_{pl} suppressed operators coupling the ‘‘observable sector’’ to the ‘‘hidden sector’’ often dominate over these contributions. Nevertheless, the chiral compensator can dominate the supersymmetry-breaking effects, for example, if the ‘‘observable’’ sector (including the supersymmetric standard model) and the ‘‘hidden sector’’ (responsible for supersymmetry breaking) reside on different branes in extra dimensions [1] or if the dynamics of the hidden sector is nearly super-conformal to suppress direct couplings between the hidden and observable fields in the Kähler potential [8]. In these cases, the only communication of supersymmetry-breaking effects from the hidden to the observable sector occurs through the supergravity multiplet, and hence the auxiliary component of the chiral compensator field. Since the coupling of the chiral compensator is completely fixed by the (fictitious) super-Weyl invariance, the consequent supersymmetry-breaking terms in the observable sector are highly constrained. This case, where the couplings between the observable and hidden sector are suppressed and the form of the SUSY breaking is highly restricted, is known generically as anomaly mediation, and it is the case which we discuss here.

If the observable sector does not have explicit mass scales, the Lagrangian is scale invariant at the classical level. Then the coupling of the chiral compensator can be completely eliminated from the Lagrangian by appropriate redefinition of the fields. However, the scale invariance is broken at the quantum level because of the need to regulate the theory. This leads to residual couplings of the chiral compensator to the observable fields. When the classical invariance of the Lagrangian is broken at the quantum level leading to physical effects, this is generically called an ‘‘anomaly.’’ This explains the name ‘‘anomaly-mediated supersymmetry breaking.’’

The implementation previously discussed in the literature uses an explicit cutoff scale Λ . Because of the imposed super-Weyl invariance, the cutoff parameter Λ only appears in the combination $\Lambda \Phi$. Such a cutoff is possible using Pauli-Villars regulators, finite $N=2$ theories [9], or higher derivative regularization [10]. Any of these methods preserve manifest supersymmetry, and the cutoff is a holomorphic parameter: The cutoff can be viewed as the lowest component of a chiral superfield. We refer to all these schemes generically as ‘‘holomorphic regularization.’’ If a holomorphic regularization scheme is used, independent of the details of the regularization method, we can derive their consequences on the supersymmetry-breaking effects in the observable fields as follows.

The matter kinetic terms receive wave function renormalization

$$\int d^4\theta \mathcal{Z}_i Q_i^* Q_i. \quad (2.1)$$

Here, \mathcal{Z}_i is the superfield extension of the wave-function renormalization, Z_i , following the formalism developed in [11,12]. \mathcal{Z}_i depends on the cutoff

$$\log \mathcal{Z}_i(\mu) = \sum_{k=1}^{\infty} C_k \log^k \frac{(\Lambda\Phi)(\Lambda\Phi)^\dagger}{\mu^2}. \quad (2.2)$$

Here, C_k are functions of dimensionless coupling constants. Expanding the logarithms in θ ,

$$\begin{aligned} \log \mathcal{Z}_i(\mu) &= \log Z_i(\mu) + (\theta^2 m_{3/2} + \bar{\theta}^2 m_{3/2}) \sum_{k=1}^{\infty} k C_k \\ &\quad \times \log^{k-1} \frac{(\Lambda\Phi)(\Lambda\Phi)^\dagger}{\mu^2} + \theta^2 \bar{\theta}^2 m_{3/2}^2 \\ &\quad \times \sum_{k=1}^{\infty} k(k-1) C_k \log^{k-2} \frac{(\Lambda\Phi)(\Lambda\Phi)^\dagger}{\mu^2} \\ &= \log Z_i(\mu) + (\theta^2 m_{3/2} + \bar{\theta}^2 m_{3/2}) \gamma_i \\ &\quad - \frac{1}{2} \theta^2 \bar{\theta}^2 m_{3/2}^2 \dot{\gamma}_i \\ &= \log Z_i(\mu) - (\theta^2 A_i + \bar{\theta}^2 A_i^*) - \theta^2 \bar{\theta}^2 m_i^2. \end{aligned} \quad (2.3)$$

Here, $\gamma = -\frac{1}{2} \mu(d/d\mu) \log Z$ and $\dot{\gamma} = \mu(d/d\mu) \gamma$. The identification of the soft terms [the last line of Eq. (2.3)] follows from rescaling the fields in Eq. (2.1) by $Q_i \rightarrow Q_i / (1 + \gamma m_{3/2} \theta^2)$. Once we note that $A_{ijk} = A_i + A_j + A_k$; this leads to the predictions in Eqs. (1.1), (1.2). As an aside, we note that both $\gamma(\mu)$ and $\dot{\gamma}(\mu)$ must be finite once reexpressed in terms of the running coupling constants at the scale μ .

The gauge coupling constant is given in terms of the bare coupling $1/g_0^2$ and the running effects in the Wilsonian effective Lagrangian as

$$\int d^2\theta \left(\frac{1}{g_0^2} + \frac{b_0}{8\pi^2} \log \frac{\Lambda\Phi}{\mu} - \sum_f \frac{T_f}{8\pi^2} \log \mathcal{Z}_i|_{\bar{\theta}=0} \right) \times W_\alpha W^\alpha. \quad (2.4)$$

By expanding the logarithms to $\mathcal{O}(\theta^2)$, we find the prediction for the holomorphic gaugino mass

$$m_\lambda(\mu) = -\frac{g_0^2}{8\pi^2} \left(b_0 - \sum_f T_f \gamma_f(\mu) \right) m_{3/2}. \quad (2.5)$$

Going to the canonical normalization of the gaugino changes the above expression to [13]

$$m_\lambda = -\frac{g^2(\mu)}{8\pi^2} \frac{b_0 - \sum_f T_f \gamma_f}{1 - \frac{g^2(\mu)}{8\pi^2} C_A} m_{3/2} = -\frac{\beta(g)}{2g^2} m_{3/2}. \quad (2.6)$$

To complete our review of established anomaly mediated results, we reemphasize that anomaly-mediation possesses

the property of ultraviolet insensitivity, namely that the effects of heavy particles completely decouple from the supersymmetry-breaking effects in the low-energy theory. With a holomorphic regularization, this is quite easy to see. Instead of logarithms dependent on μ , as in Eq. (2.2), loop effects of a heavy particle cutoff at its mass M and so appear with the logarithms

$$\log \frac{(\Lambda\Phi)(\Lambda\Phi)^\dagger}{(M\Phi)(M\Phi)^\dagger} = \log \frac{\Lambda^2}{M^2}. \quad (2.7)$$

The point here is that the super-Weyl invariance makes the mass M appear only in the combination $M\Phi$ which precisely cancels the corresponding Φ dependence of the cutoff. Therefore there are no supersymmetry-breaking effects from heavy particles in the low-energy theory. We will now attempt to understand this ultraviolet insensitivity explicitly in the DRED formalism as well.

III. DRED-FUL UV SENSITIVITY?

In this section we will outline a naive DRED calculation. We will find that simply adding the anomaly-mediated soft terms of Eqs. (1.1) and (1.2) to our Lagrangian by hand and then calculating using DRED leads to inconsistencies. In particular, we are unable to recover the well-established result of UV insensitivity. In this section we demonstrate the problem using the technique of Arkani-Hamed, Giudice, Luty and Rattazzi [11] which ‘‘analytically continues’’ parameters in the Lagrangian to the full superspace to incorporate the effects of soft supersymmetry breaking. We will do explicit diagrammatic calculations in later sections to further illuminate this problem.

Consider a simple Yukawa model

$$\mathcal{W} = h \tau X_1 X_2 + M X_1 Y_1 + M X_2 Y_2, \quad (3.1)$$

where τ is a light field and X_i, Y_i heavy. The massive fields have tree-level supersymmetry breaking because the chiral compensator appears in the superpotential as $M\Phi$:

$$\mathcal{L}_{soft} = -M m_{3/2} (\bar{X}_1 \bar{Y}_1 + \bar{X}_2 \bar{Y}_2) + \text{H.c.} \quad (3.2)$$

In addition, there are anomaly-mediated effects according to the general formula of Eqs. (1.1), (1.2),

$$\begin{aligned} \mathcal{L}_{soft} &= -3 \frac{(h^* h)^2}{(4\pi)^4} m_{3/2} (\tilde{\tau}^* \tau + \tilde{X}_1^* \tilde{X}_1 + \tilde{X}_2^* \tilde{X}_2) \\ &\quad - 3 \frac{h^* h}{(4\pi)^2} m_{3/2} h \tilde{\tau} \tilde{X}_1 \tilde{X}_2 + \text{H.c.} \end{aligned} \quad (3.3)$$

The question of ultraviolet insensitivity is whether the scalar mass for the $\tilde{\tau}$ shown in Eq. (3.3) is precisely canceled by the threshold effects from X, Y loops.

As we will describe in detail in Sec. IX, the loops of X and Y precisely cancel $m_{\tilde{\tau}}^2$ if all integrals are done in four dimensions, paying careful attention to keep all integrals finite. However, we can also understand this computation

rather simply using the language of the spurions. First, we compute the Z factor for τ at $Q^2 \gg M^2$. It is given by

$$\log Z_\tau(Q) = \frac{h^*h}{(4\pi)^2} \log \frac{|\Lambda|^2}{Q^2} - \frac{(h^*h)^2}{(4\pi)^4} \frac{3}{2} \log^2 \frac{|\Lambda|^2}{Q^2}. \quad (3.4)$$

Now, we incorporate supersymmetry-breaking effects by substituting $\Lambda \rightarrow \Lambda\Phi$. Performing this replacement, and inserting the vacuum expectation value for the chiral compensator, $\langle \Phi \rangle = 1 + m_{3/2}\theta^2$, we obtain the anomaly-mediated pieces shown in Eq. (3.3). Now we integrate between the scale Q and M and find the low-energy theory below M . The additional contribution to Z_τ is

$$\Delta \log Z_\tau = \frac{h^*h}{(4\pi)^2} \log \frac{Q^2}{M^2} - \frac{(h^*h)^2}{(4\pi)^4} \frac{3}{2} \log^2 \frac{Q^2}{M^2}. \quad (3.5)$$

Using this expression, we can isolate the supersymmetry-breaking effects in the threshold correction.

One effect arises from taking $M \rightarrow M\Phi$ in the last term, which gives $\Delta m_\tau^2 = +3[(h^*h)^2/(4\pi)^4]m_{3/2}^2$. This corresponds to the sum of all two-loop diagrams in Figs. 5 and 6 with $-Mm_{3/2}\tilde{X}_i\tilde{Y}_i$ mass insertions. The other source of SUSY breaking is the A term. Its effects can be obtained by the replacement $h \rightarrow h\{1 - 3[h^2/(4\pi)^2]m_{3/2}\theta^2\}$ together with $M \rightarrow M\Phi$ in the first term (and a similar replacement for h^*). The contribution to Δm_τ^2 is $-6[(h^*h)^2/(4\pi)^4]m_{3/2}^2$. This corresponds to the one-loop diagram, Graph 7-1, that contains one A term and one $Mm_{3/2}$ mass insertion. Adding the threshold corrections to the anomaly-mediated piece $+3[(h^*h)^2/(4\pi)^4]m_{3/2}^2$, we find a complete cancellation. This cancellation demonstrates the UV insensitivity.

Now we perform the same calculations, using regularization by dimensional reduction (DRED), and we do not find the complete cancellation. The threshold correction can again be read off from the Z factor

$$\Delta \log Z_\tau = \frac{h^*h}{(4\pi)^2} (M^{-2\epsilon} - Q^{-2\epsilon}) \frac{1}{\epsilon} - \frac{(h^*h)^2}{(4\pi)^4} \frac{3}{2} (M^{-4\epsilon} - Q^{-4\epsilon}) \frac{1}{\epsilon^2}. \quad (3.6)$$

Suppose we do the calculation in the same spirit as in the case with the holomorphic regularization. Then, we should again include contributions from two sources: a cross term between an A term and the $Mm_{3/2}$ term, shown in Graph 7-1, and the diagrams including only the $Mm_{3/2}$ term. The contribution from the A term and $M\Phi$ in Graph 7-1 can be found again by making the replacement $h \rightarrow h\{1 - 3[h^2/(2\pi)^2]m_{3/2}\theta^2\}$ together with $M \rightarrow M\Phi$ in the first term of Eq. (3.6). The result is the same as in the holomorphic regularization: $\Delta m_\tau^2 = -6[(h^*h)^2/(4\pi)^4]m_{3/2}^2$. However, the other contribution from the replacement $M \rightarrow M\Phi$ in the last term of Eq. (3.6) comes out differently. Because

$$(M^2\Phi\bar{\Phi})^{-2\epsilon} = (M^2)^{-2\epsilon} (1 - 2\epsilon\theta^2 m_{3/2} - 2\epsilon\bar{\theta}^2 m_{3/2} + 4\epsilon^2\theta^2\bar{\theta}^2 m_{3/2}^2),$$

we find $\Delta m_\tau^2 = +6[(h^*h)^2/(4\pi)^4]m_{3/2}^2$. Summing this result with the contribution from the A terms, we find $\Delta m_\tau^2 = 0$. We will explore in detail how this result, which differs from the holomorphic regularization result, arises in Sec. IX. For now, the important thing is to realize that we have found an unexpected result. We had hoped to find a threshold correction, that when added to the anomaly mediated piece, $+3[(h^*h)^2/(4\pi)^4]m_{3/2}^2$, would yield a complete cancellation. Instead, we find that the ‘‘threshold correction’’ itself vanishes. Somehow we seem to have lost the ultraviolet insensitivity.²

What we have seen here is that the naive addition of the anomaly-mediated supersymmetry-breaking soft terms to a dimensionally-reduced theory leads to incorrect results. That is to say, putting the terms from Eqs. (1.1) and (1.2) in the Lagrangian by hand is *not* the correct prescription in DRED. Note that most calculations in the literature are done with this naive implementation. We have to develop a consistent formalism to implement anomaly-mediated supersymmetry breaking within the DRED. We proceed to do this in the following section.

Finally, we comment on the reason that things did not ‘‘go wrong’’ in the holomorphic regularization scheme. In that case, one has already integrated out the fictitious Pauli-Villars fields at the cutoff scale, yielding the anomaly-mediated soft terms of Eqs. (1.1) and (1.2) at the cutoff scale. Therefore, in the Pauli-Villars case, it is perfectly reasonable to treat the usual anomaly-mediated soft terms as a boundary condition at the cutoff scale. We will expand upon this point in Sec. VI.

IV. DERIVATION OF THE LAGRANGIAN IN DIMENSIONAL REDUCTION

In this section we motivate the bare Lagrangians appropriate for use with DRED regularization. We look at both the case of a Yukawa theory and a theory with gauge couplings, trusting that combining the two provides no new wrinkles. In each case, our procedure basically consists of starting with a supersymmetric Lagrangian, and determining how chiral compensators inject supersymmetry breaking into the Lagrangian.

By examining the Weyl scaling properties of the supergravity fields, we can determine where we must add chiral compensator fields Φ to the supergravity Lagrangian to make it super-Weyl invariant. As noted above, we can then rescale fields so that the chiral compensator appears only in front of dimensional couplings. This fixes how supersymmetry breaking enters the Lagrangian since the breaking hap-

²In fact, there is an additional piece that comes in at h^2 proportional to ϵ . The presence of this term does not change the fact that we have gotten an unexpected result.

pens when Φ takes the vacuum expectation value $\Phi = 1 + m_{3/2}\theta^2$.

Here is how this works for a dimensionally reduced theory with Yukawa couplings: In $4 - 2\epsilon$ dimensions, the Lagrangian, written in terms of bare chiral superfields looks like

$$\mathcal{L} = \int d^4\theta (\Phi\Phi^\dagger)^{1-\epsilon} Q_i^\dagger Q_i - \left(\int d^2\theta \Phi^{3-2\epsilon} (\lambda_{ijk,0} Q_i Q_j Q_k + M_{ij,0} Q_i Q_j) + \text{H.c.} \right). \quad (4.1)$$

Here, the 0 subscript denotes a bare quantity. To recover canonical normalization, we rescale

$$Q_i \rightarrow \frac{Q_i}{\Phi^{1-\epsilon}}, \quad (4.2)$$

and then as promised, the chiral compensators only appear in front of dimensionful couplings in the superpotential:

$$\mathcal{L} = \int d^4\theta Q_i^\dagger Q_i - \left(\int d^2\theta \Phi^\epsilon \lambda_{ijk,0} Q_i Q_j Q_k + \Phi M_{ij,0} Q_i Q_j + \text{H.c.} \right). \quad (4.3)$$

The extra power of Φ^ϵ can be thought of as arising from the ϵ dimensionality of $\lambda_{ijk,0}$ which appears in $4 - 2\epsilon$ dimensions. Expanding in components, we find two sources of supersymmetry breaking in the bare Lagrangian:

$$\mathcal{L}_{\text{breaking}} \ni -\epsilon m_{3/2} \lambda_{ijk,0} \tilde{Q}_i \tilde{Q}_j \tilde{Q}_k - m_{3/2} M_{ij,0} \tilde{Q}_i \tilde{Q}_j. \quad (4.4)$$

The first term is one of the important evanescent operators which produces anomaly-mediated soft terms to the low-energy effective Lagrangian.

For the gauge theory we begin with the Lagrangian

$$\mathcal{L} \ni \frac{1}{4g_0^2} \int d^2\theta WW + \frac{1}{4g_0^2} \int d^2\bar{\theta} \bar{W} \bar{W} \quad (4.5)$$

and dimensionally reduce it. The Φ dependence can be fixed by arguments of holomorphicity and dimensionality, in analogy with the resulting $\Phi^\epsilon \lambda_{ijk,0}$ dependence found above. Then we should promote $1/g_0^2$ to a superfield gauge coupling [11,12],

$$\frac{1}{g_0^2} \rightarrow S = \frac{\Phi^{-2\epsilon}}{g_0^2}, \quad (4.6)$$

with which the Lagrangian becomes

$$\mathcal{L} \ni \frac{1}{4} \int d^2\theta SWW + \frac{1}{4} \int d^2\bar{\theta} S^\dagger \bar{W} \bar{W}. \quad (4.7)$$

We then would like to associate a real superfield, R_0 , with the gauge coupling constant [11]. With the above Lagrangian, the superfield R_0 , whose lowest component is $1/g_0^2$, is given by

$$R_0 \equiv \frac{\Phi^{-2\epsilon} + (\Phi^\dagger)^{-2\epsilon}}{2g_0^2}. \quad (4.8)$$

However, this choice does not lead to the familiar prediction of the anomaly-mediated supersymmetry breaking: $m^2 = \frac{1}{2} \dot{\gamma} m_{3/2}^2$. It differs at $O(\epsilon)$. We will work with a more convenient form that leads to the familiar prediction without $O(\epsilon)$ corrections. Instead of Eq. (4.8) we take

$$R_0 \equiv \frac{(\Phi\Phi^\dagger)^{-\epsilon}}{g_0^2}. \quad (4.9)$$

The two expressions for R_0 differ only in $\theta^2 \bar{\theta}^2$ components, which does not lead to any physical difference in the four-dimensional limit. We prove this fact in the next section.

Using Eq. (4.9) as the real gauge coupling superfield, we can write the bare Lagrangian using the Grisaru-Milewski-Zanon (GMZ) evanescent operator [14]. Here the bare action is given by

$$\frac{1}{g_0^2} \int d^8z \frac{1}{\epsilon} (\Phi\Phi^\dagger)^{-\epsilon} g_\epsilon^{\mu\nu} \text{tr}(\Gamma_\mu \Gamma_\nu). \quad (4.10)$$

The metric tensor $g_\epsilon^{\mu\nu}$ runs only for the compactified 2ϵ dimensions, and Γ_μ is the gauge connection defined by

$$\Gamma^\mu = \frac{1}{2} \sigma_{\alpha\dot{\alpha}}^\mu \bar{D}^{\dot{\alpha}} (e^{-V} D^\alpha e^V). \quad (4.11)$$

This leads to a component Lagrangian that contains the following supersymmetry-breaking pieces:

$$\mathcal{L}_{\text{breaking}} \ni \frac{1}{g_0^2} \left(\frac{1}{2} \epsilon m_{3/2} \lambda \lambda + \frac{1}{2} \epsilon m_{3/2} \bar{\lambda} \bar{\lambda} + \frac{\epsilon}{2} m_{3/2}^2 g_\epsilon^{\mu\nu} A_\mu A_\nu \right). \quad (4.12)$$

Therefore, the supersymmetry-breaking effects are a tree-level $\mathcal{O}(\epsilon)$ gaugino mass $m_\lambda = -\epsilon m_{3/2}$, and a tree-level ϵ -scalar mass $m_\epsilon^2 = \epsilon m_{3/2}^2$.

For Abelian theories, we may also use

$$\frac{1}{16g_0^2} \int d^4\theta (\Phi\Phi^\dagger)^{-\epsilon} W^\alpha \frac{\mathcal{D}^2}{\square} W_\alpha + \text{H.c.} \quad (4.13)$$

to introduce the real superfield gauge coupling, Eq. (4.9). In this framework the ϵ -scalar mass is replaced by a non-local modification of the gaugino propagator. We find

$$\mathcal{L}_{\text{breaking}} \ni \frac{1}{g_0^2} \left[\frac{1}{2} \epsilon m_{3/2} \lambda \lambda + \frac{1}{2} \epsilon m_{3/2} \bar{\lambda} \bar{\lambda} + \frac{1}{2} \epsilon^2 m_{3/2}^2 \left(-i \frac{\lambda \sigma \cdot \partial \bar{\lambda}}{\square} \right) \right]. \quad (4.14)$$

However, it is not clear how to interpret a non-local term in a bare Lagrangian. Moreover, an extension to non-Abelian theories is somewhat opaque due to difficulties in making the expression containing $1/\square$ gauge covariant. Nevertheless, it provides a useful cross-check to our calculations with the GMZ operator in an Abelian gauge theory.

V. DERIVATION OF THE SOFT SUPERSYMMETRY-BREAKING TERMS IN DRED

With bare Lagrangians in hand, we now go back and derive the anomaly mediation formulas for the soft supersymmetry-breaking parameters [Eqs. (1.1) and (1.2)] for DRED regularization. This discussion is to be compared with the known discussion for holomorphic regulators, reviewed in Sec. II.

A. Yukawa theory

In the Yukawa theory the bare Lagrangian is given by Eq. (4.3). For simplicity in this section we drop the mass terms, so that

$$\mathcal{L} = \int d^4 \theta Q_i^\dagger Q_i - \left(\int d^2 \theta \Phi^\epsilon \lambda_{ijk,0} Q_i Q_j Q_k + \text{H.c.} \right). \quad (5.1)$$

The important point is that $\Phi^\epsilon \lambda_{ijk,0}$ acts as an effective Yukawa coupling constant.

We start by considering the wave-function renormalization³ Z that appears in the effective Lagrangian. Again, following the discussion of [11,12], we promote Z to a superfield \mathcal{Z} , and we expand in a power series of effective coupling constants $\Phi^\epsilon \lambda_{ijk,0}$:

$$\log \mathcal{Z}(\mu) = \sum_{k=1}^{\infty} \frac{D_k}{\epsilon^k} \left(\frac{\lambda_{ijk,0} \lambda_{ijk,0}^* (\Phi \Phi^\dagger)^\epsilon}{\mu^{2\epsilon}} \right)^k. \quad (5.2)$$

The coefficients D_k are regular in the $\epsilon \rightarrow 0$ limit. Since the Yukawa coupling in $4-2\epsilon$ dimensions is dimensionful, it appears always with an appropriate factor of Φ^ϵ .

Now we expand the chiral compensator $\Phi = 1 + m_{3/2} \theta^2$, yielding the expression

$$\begin{aligned} \log \mathcal{Z} = & \sum_{k=1}^{\infty} \frac{D_k}{\epsilon^k} \left(\frac{\lambda_{ijk,0} \lambda_{ijk,0}^*}{\mu^{2\epsilon}} \right)^k \\ & + \sum_{k=1}^{\infty} \frac{(m_{3/2} \theta^2 + \text{H.c.}) k D_k}{\epsilon^{k-1}} \left(\frac{\lambda_{ijk,0} \lambda_{ijk,0}^*}{\mu^{2\epsilon}} \right)^k \\ & + \sum_{k=1}^{\infty} \frac{m_{3/2}^2 \theta^2 \bar{\theta}^2 k^2 D_k}{\epsilon^{k-2}} \left(\frac{\lambda_{ijk,0} \lambda_{ijk,0}^*}{\mu^{2\epsilon}} \right)^k. \end{aligned} \quad (5.3)$$

Finally, we can write the expressions for γ and $\dot{\gamma}$ by taking the appropriate derivatives of the first term in Eq. (5.3). We find

$$\gamma = \sum_{k=1}^{\infty} \frac{k D_k}{\epsilon^{k-1}} \left(\frac{\lambda_{ijk,0} \lambda_{ijk,0}^*}{\mu^{2\epsilon}} \right)^k, \quad (5.4)$$

$$\dot{\gamma} = -2 \sum_{k=1}^{\infty} \frac{k^2 D_k}{\epsilon^{k-2}} \left(\frac{\lambda_{ijk,0} \lambda_{ijk,0}^*}{\mu^{2\epsilon}} \right)^k. \quad (5.5)$$

Now using Eqs. (5.3), (5.4), and summing the contributions from the i, j , and k particles, we find

$$\begin{aligned} \mathcal{L} = & \int d^4 \theta \left(1 - \frac{\dot{\gamma}_i}{2} m_{3/2}^2 \theta^2 \bar{\theta}^2 \right) Q_i^\dagger Q_i - \int d^2 \theta \lambda_{ijk} \Phi^\epsilon \\ & \times [1 - (\gamma_i + \gamma_j + \gamma_k) m_{3/2} \theta^2] Q_i Q_j Q_k + \text{H.c.}, \end{aligned} \quad (5.6)$$

where we distinguish the renormalized Yukawa coupling by $\lambda_{ijk} \equiv \lambda_{ijk,0} Z_i^{-1/2} Z_j^{-1/2} Z_k^{-1/2}$. The soft terms do indeed take the form of Eq. (1.1) and Eq. (1.2). Notice, however, that an additional $O(\epsilon)$ supersymmetry-breaking Yukawa coupling arises by expanding Φ^ϵ . This is just the tree-level evanescent operator from the bare Lagrangian as in Eq. (4.4). Our effective Lagrangian contains a total A term

$$A_{ijk} = -m_{3/2} \lambda_{ijk} (\gamma_i + \gamma_j + \gamma_k) + \epsilon m_{3/2} \lambda_{ijk}. \quad (5.7)$$

B. Gauge theory

If we turn off the Yukawa theory but add gauge interactions, the discussion proceeds analogously. Instead of the effective Yukawa coupling $\Phi^\epsilon \lambda_{ijk,0}$, the relevant expansion parameter for \mathcal{Z} is $g_0^2 (\Phi \Phi^\dagger)^\epsilon$. This is clear from Eqs. (4.10), (4.13). Now we justify the form of Eq. (4.9). To do this, we need to show that there is no physical consequence in switching from Eqs. (4.8) to (4.9) in the four-dimensional limit.

Consider the following change in the real gauge-coupling superfield:

$$R \rightarrow R + \theta^2 \bar{\theta}^2 \frac{\Delta^2}{g^2}. \quad (5.8)$$

Clearly this change will not affect one-loop quantities such as A terms and the gaugino mass, as both of these depend solely on the θ^2 pieces of the Lagrangian. We show now that

³Note that in our notation, Z^{-1} is the residue of the pole that one would find by calculating the two-point function. That is to say, Z would be the coefficient of the bare fields QQ^\dagger in the one particle irreducible (1PI) effective action.

the scalar masses are also unaffected in the four dimensional-limit as we pass from Eq. (4.8) to Eq. (4.9).

The argument is simple. (To keep our expressions uncluttered we work with a single gauge coupling constant, but we have checked that the argument can be generalized to multi-coupling theories.) Generally, under the transformation of R in Eq. (5.8), the change in the mass-squared of a matter field Q_i is

$$m_i^2 \rightarrow m_i^2 + \frac{\gamma_i}{\epsilon} \Delta^2. \quad (5.9)$$

We can see this as follows. Starting from the expansion

$$\log Z_i = \sum_{k=1}^{\infty} C_k g_0^{2k} \mu^{-2k\epsilon}, \quad (5.10)$$

we find

$$\gamma_i = \epsilon \sum_{k=1}^{\infty} k C_k g_0^{2k} \mu^{-2k\epsilon}. \quad (5.11)$$

Now, the change in R above is the same as the replacement

$$R^{-1} \rightarrow R^{-1} (1 - \theta^2 \bar{\theta}^2 \Delta^2). \quad (5.12)$$

Recall that to recover the scalar masses, we need the $\theta^2 \bar{\theta}^2$ piece of $\log \mathcal{Z}$, which is found by replacing g_0^2 in Eq. (5.10) by R^{-1} . So the change in R^{-1} induces a change in $\theta^2 \bar{\theta}^2$ component of $\log \mathcal{Z}_i$ as given by making the replacement

$$g_0^2 \rightarrow R^{-1} (1 - \theta^2 \bar{\theta}^2 \Delta^2) \quad (5.13)$$

in Eq. (5.10). Therefore the change in $m_i^2 = -\log \mathcal{Z}_i|_{\theta^2 \bar{\theta}^2}$ is

$$\Delta m_i^2 = - \sum_{k=1}^{\infty} C_k g_0^{2k} (-k \Delta^2) \mu^{-2k\epsilon} = \frac{\gamma_i}{\epsilon} \Delta^2. \quad (5.14)$$

This proves the assertion of Eq. (5.9). Now notice that the difference between

$$R_1 = \frac{g_0^{-2} (\Phi^{-2\epsilon} + \Phi^{\dagger -2\epsilon})}{2} \quad (5.15)$$

and

$$R_2 = g_0^{-2} (\Phi \Phi^\dagger)^{-\epsilon}, \quad (5.16)$$

is $\Delta^2 \equiv R_1 - R_2 = -\epsilon^2 m_{3/2}^2$. Therefore, in this case, the change in the scalar masses is only $\mathcal{O}(\epsilon)$ and does not affect the 4-dimensional limit.

Now that the choice $R_2^{-1} = g_0^2 (\Phi \Phi^\dagger)^\epsilon$ is justified, the derivation of the soft parameters follows the same path as in the Yukawa theory. Incidentally, our argument shows that we are performing a calculation in the dimensional reduction with modified numerical subtraction ($\overline{\text{DR}'}$) scheme [15]. We have calculated the above-threshold case with a finite external momentum. In particular, we can always take the value of this momentum to be on-shell. Then there is no additional

change that depends on the ϵ -scalar mass in going from the $m^2(\mu)$ we have calculated to the pole mass. By definition, this is the $\overline{\text{DR}'}$ scheme. This is consistent with the comments found in [11].

We can also derive the gaugino mass following the same line, even though it was already discussed in [2]. The effective action is

$$\int d^8 z R(\mu) \frac{1}{\epsilon} (\Phi \Phi^\dagger)^{-\epsilon} g_\epsilon^{\mu\nu} \text{tr}(\Gamma_\mu \Gamma_\nu), \quad (5.17)$$

where the lowest order in $R(\mu)$ is the renormalized coupling $g^2(\mu) \mu^{-2\epsilon}$. We now define a dimensionless superfield, $\mathcal{F}(\mu)$, such that $g^2(\mu) = \mathcal{F}^{-1}(\mu)|_{\theta=\bar{\theta}=0}$. The kinetic function is a function of the bare coupling g_0 together with the chiral compensator as

$$\mathcal{F}(g_0^2 \mu^{-2\epsilon} (\Phi \Phi^\dagger)^\epsilon). \quad (5.18)$$

Expanding the function \mathcal{F} , we find

$$\begin{aligned} \mathcal{F}(\mu) &= \frac{1}{g^2(\mu)} + \mathcal{F}' \Big|_{\theta=\bar{\theta}=0} g_0^2 \mu^{-2\epsilon} \epsilon (\theta^2 + \bar{\theta}^2) m_{3/2} \\ &+ (\mathcal{F}' g_0^2 \mu^{-2\epsilon} + \mathcal{F}'' g_0^4 \mu^{-4\epsilon})_{\theta=\bar{\theta}=0} \epsilon^2 \bar{\theta}^2 \theta^2 m_{3/2}^2. \end{aligned} \quad (5.19)$$

Noting that

$$\beta(g) = \mu \frac{d}{d\mu} \mathcal{F}^{-1} \Big|_{\theta=\bar{\theta}=0} = -2\epsilon g_0^2 \mu^{-2\epsilon} \frac{-1}{\mathcal{F}^2} \mathcal{F}' \Big|_{\theta=\bar{\theta}=0}, \quad (5.20)$$

we find

$$g_0^2 \mu^{-2\epsilon} \epsilon \mathcal{F}' \Big|_{\theta=\bar{\theta}=0} = \frac{\beta(g)}{2g^4(\mu)}. \quad (5.21)$$

Furthermore, differentiating it on both sides,

$$\begin{aligned} &-2\epsilon^2 (\mathcal{F}' g_0^2 \mu^{-2\epsilon} + \mathcal{F}'' g_0^4 \mu^{-4\epsilon})_{\theta=\bar{\theta}=0} \\ &= \mu \frac{d}{d\mu} \frac{\beta(g)}{2g^4(\mu)} \\ &= \frac{\dot{\beta}(g)}{2g^4(\mu)} - 2 \frac{\beta^2(g)}{2g^6(\mu)}. \end{aligned} \quad (5.22)$$

Here, $\dot{\beta}(g) = \mu(d/d\mu)\beta(g)$. Therefore,

$$\begin{aligned} \mathcal{F}(\mu) &= \frac{1}{g^2(\mu)} + \frac{\beta(g)}{2g^4(\mu)} (\theta^2 + \bar{\theta}^2) m_{3/2} \\ &- \frac{1}{2} \mu \frac{d}{d\mu} \frac{\beta(g)}{2g^4(\mu)} \theta^2 \bar{\theta}^2 m_{3/2}^2. \end{aligned} \quad (5.23)$$

We therefore find the gaugino mass

$$m_\lambda = -\frac{\beta(g)}{2g^2(\mu)} m_{3/2}, \quad (5.24)$$

consistent with the derivation in [2]. We also find an all-order result for the epsilon scalar mass

$$m_\epsilon^2 = -\frac{1}{2} g^2(\mu) \mu \frac{d}{d\mu} \frac{\beta(g)}{2g^4(\mu)} m_{3/2}^2 \quad (5.25)$$

which had not been obtained in the literature. It would be interesting to verify explicitly that this result is on the renormalization-group trajectory in the manner of Ref. [7].

VI. MORAL

The important moral to be taken away from the last three sections is the following: in DRED anomaly-mediated supersymmetry-breaking effects are to be *calculated* from the bare Lagrangian, and cannot be added to the Lagrangian by hand. The basic mistake in the naive calculation in Sec. III is that we added the ‘‘anomaly-mediated supersymmetry breaking’’ to the Lagrangian by hand and tried to demonstrate the UV insensitivity with this cobbled together Lagrangian. The reason why this is a mistake is clear from the analogy to the chiral anomaly mentioned in the Introduction. In a regularized theory, the chiral anomaly comes out automatically from the loop calculations. One does not add the chiral anomaly as an additional term to the Lagrangian. In the same way, DRED is a regularization, which leads automatically to the anomaly-mediated supersymmetry breaking. Therefore, instead of adding soft parameters to the Lagrangian, we should perform a complete calculation starting from the bare Lagrangian that contains a Yukawa coupling $\lambda_0 \Phi^\epsilon$ or a gauge coupling $g_0^2 (\Phi \Phi^\dagger)^\epsilon$. Then we should find that contributions of heavy multiplets to the soft couplings vanish below the heavy mass threshold. We illustrate this UV insensitivity using DRED in our diagrammatic calculation of Sec. IX.

Finally, let us enhance this discussion by describing the proof of ultraviolet insensitivity in anomaly mediation with the DRED framework. This is the analogue of Eq. (2.7). In general, the contributions from heavy multiplets to the Z factor have the dependence $(\lambda * \lambda)^k (M * M)^{-k\epsilon}$. The correct inclusion of the chiral compensator then gives $(\lambda \Phi^\epsilon \lambda * \Phi^\dagger \epsilon)^k (M \Phi M * \Phi^\dagger)^{-k\epsilon} = (\lambda * \lambda)^k (M * M)^{-k\epsilon}$, and no supersymmetry-breaking effects remain.

Now we can analyze what went wrong in our example in Sec. III. Operationally, we made two errors in our calculation. First of all, we extended the Yukawa coupling incorrectly. Instead of extending it to get the A -term diagram through the replacement $h \rightarrow h\{1 - 3[h^2/(4\pi)^2]m_{3/2}\theta^2\}$, we were meant to make the replacement $h \rightarrow h\Phi^\epsilon$. Moreover, we neglected a one-loop $\mathcal{O}(\epsilon h^2)$ piece that was present in the high-energy theory. In fact, in our attempt to compute the threshold correction to $\log Z$, we ended up computing the entirety of $\log Z$. We were unable to separate the high-energy piece from the threshold correction.

The above discussion seems to say that it is impossible to regard the anomaly-mediated supersymmetry breaking as a boundary at the Planck scale. Indeed, this appears to be true for DRED. However, this is not impossible for other regularization schemes. We can take this view, for instance, if we use Pauli-Villars regulators where the supersymmetry-breaking $\Lambda m_{3/2}$ mass term for the regulators is the source of all other supersymmetry-breaking effects. Then we can play the following trick. We add a pair of correct- and wrong-statistics regulator fields without $\Lambda m_{3/2}$ mass term, which does not change the physics at all. Then we integrate out the original Pauli-Villars regulators with the $\Lambda m_{3/2}$ mass term and a correct-statistics field without the $\Lambda m_{3/2}$ mass term. Integrating out this pair of fields will give us the soft SUSY-breaking terms of Eqs. (1.1) and (1.2), where the anomalous dimensions are to be evaluated at the cut-off scale. The left-over wrong-statistics massive field acts as the new Pauli-Villars regulator while the supersymmetry-breaking effects are now in the Lagrangian. This way, we obtain an entirely equivalent theory with anomaly-mediated supersymmetry breaking in the bare Lagrangian, regulated by the Pauli-Villars regulators that do not have a $\Lambda m_{3/2}$ mass term. On the other hand, DRED does not allow us a similar trick because there is no ‘‘regulator field.’’ We need to keep evanescent operators consistently in calculations.

In later sections, we will study the UV insensitivity with explicit diagrammatic calculations. The situation can be somewhat more subtle in the presence of both light and heavy degrees of freedom, but nonetheless we have demonstrated that the effects of heavy multiplets completely disappear from the soft supersymmetry-breaking parameters below the heavy threshold once coupling constants are reexpressed in terms of renormalized ones.

VII. MODEL CONSIDERED

We now define two simple toy models to satisfy the diagrammatic computation promised in the previous sections. Calculations using these models will follow in Secs. VIII and IX.

The first model contains only chiral superfields with minimal kinetic terms and superpotential

$$\mathcal{W}_1 = \lambda_{\tau,0} \tau L H + h_0 \tau X_1 X_2 + M X_1 Y_1 + M X_2 Y_2. \quad (7.1)$$

(Note $\mathcal{L} \ni -\mathcal{W}_1$.) Our notation τ, L, H indicates that we are thinking of these as the essentially massless tau, lepton doublet, and down-type Higgs doublet superfields of the minimal supersymmetric standard model (MSSM), with λ_τ the usual MSSM Yukawa coupling. Here X_1, X_2, Y_1, Y_2 are the heavy fields which have flavor-dependent couplings, i.e. they only couple to the τ superfield. h is a Yukawa coupling and M is a supersymmetry-preserving heavy mass. As discussed in the previous sections, we should add a chiral compensator Φ in front of mass terms and a factor Φ^ϵ in front of Yukawa couplings. Note that all gauge interactions have been turned off in this model.

In the second model we turn off all Yukawa couplings but add an Abelian gauge coupling which one can think of as a

new $U(1)$ flavor-dependent gauge interaction with gauge coupling g' . The superpotential now only serves to make the flavor fields heavy:

$$\mathcal{W}_2 = M X_1 Y_1 + M X_2 Y_2, \quad (7.2)$$

and again chiral compensators must be added in front of masses. We keep the τ particle in the second model but drop L and H .

The aim of this exercise is twofold. First of all, we have a chance to display how anomaly-mediated calculations proceed in dimensional reduction. Second, we will show how integrating heavy X and Y superfields gives rise to the threshold effects that precisely maintain the anomaly-mediation form for the scalar masses. As mentioned previously, this diagrammatic approach is completely complementary to the already established approach of the spurion calculus.

To demonstrate the decoupling, we will calculate quantities ‘‘above threshold’’ and ‘‘below threshold.’’ Above threshold we are calculating quantities with finite external momenta well above the mass M . In these calculations, we neglect this mass relative to momenta. Below threshold, we can neglect the external momentum relative to the masses. This is the energy regime where we expect to see the dependence on the X and Y vanish.

VIII. A TERMS

In this section we explicitly demonstrate the ultraviolet insensitivity of the A terms associated with the τLH operator of Eq. (7.1). This affords us our first opportunity to see how operators proportional to ϵ are vital to our understanding of supersymmetry breaking in anomaly mediation. We calculate in bare perturbation theory and use the mass-insertion formalism, which allows us easily to pinpoint the contributions that arise at lowest order in the gravitino mass.

Recalling Eq. (1.1),

$$A_{\tau LH} = -m_{3/2} \lambda_\tau (\gamma_\tau + \gamma_L + \gamma_H). \quad (8.1)$$

Now, γ_τ changes as we integrate out the X and Y flavor superfields, and we expect to see this difference in computing the 3-point $\tilde{\tau} \tilde{L} H$ function above and below threshold. $A_{\tau LH}$ maintains the form of Eq. (8.1) even though its value changes.

In the literature anomalous dimensions are typically quoted in terms of the renormalized or running couplings $\lambda_\tau(\mu)$ and $h(\mu)$ at momentum scale μ . Here we have

$$\gamma_\tau(\mu)_{\text{above threshold}} = \frac{1}{(4\pi)^2} [2\lambda_\tau \lambda_\tau^*(\mu) + hh^*(\mu)], \quad (8.2)$$

$$\gamma_\tau(\mu)_{\text{below threshold}} = \frac{1}{(4\pi)^2} [2\lambda_\tau \lambda_\tau^*(\mu)], \quad (8.3)$$

where factors of two in front of λ_τ reflect the fact that L and H are doublet fields. To one-loop the running couplings and bare couplings are identical, so we can freely compare these

expressions with the 3-point $\tilde{\tau} \tilde{L} H$ function computed in bare perturbation theory. In the two-loop scalar mass-squared computation, however, we will need to distinguish between bare and renormalized couplings.

In the expressions for γ_τ we see explicitly the ultraviolet insensitivity: Above threshold the heavy particles contribute $h^* h / (4\pi)^2$ to γ_τ or $-m_{3/2} \lambda_\tau h^* h / (4\pi)^2$ to $A_{\tau LH}$. Below threshold they do not contribute at all: The soft supersymmetry-breaking parameter $A_{\tau LH}$ is independent of the heavy-field Yukawa parameter h . Our task now is to confirm this by diagrammatic calculation.

The relevant diagrams appear in Fig. 1. (The mass insertion proportional to $M m_{3/2}$ is indicated by a cross on the $\tilde{Y} \tilde{X}$ scalar line.) Above threshold at scale μ , Graph 1-1 vanishes quadratically in M^2/μ^2 , so we ignore it. This leaves Graph 1-2 which has value

$$\text{Graph 1-2} = i \frac{m_{3/2} h_0 h_0^* \lambda_{\tau,0}}{(4\pi)^2}, \quad (8.4)$$

exactly the contribution to $A_{\tau LH}$ expected from Eqs. (8.1) and (8.2).⁴ As anticipated in Sec. II, the graph with the evanescent ϵ operator produces the anomaly-mediated contribution to the A term. A graph analogous to Graph 1-2 with L and H fields running in the loop contributes the $\lambda_\tau^* \lambda_\tau^2$ piece to the A term coupling.

When $\mu \ll M$, we find an additional contribution from integrating out the X and Y fields, which is Graph 1-1:

$$\text{Graph 1-1} = -i \frac{m_{3/2} h_0 h_0^* \lambda_{\tau,0}}{(4\pi)^2}. \quad (8.5)$$

As promised, this is equal and opposite to the contribution from the ϵ operator. Together, Graph 1-1 + Graph 1-2 = 0, so that at scales $\mu \ll M$ below threshold, the flavor-dependent interactions of the heavy particles do not contribute to the A -term coupling. This bears out Eq. (8.3).

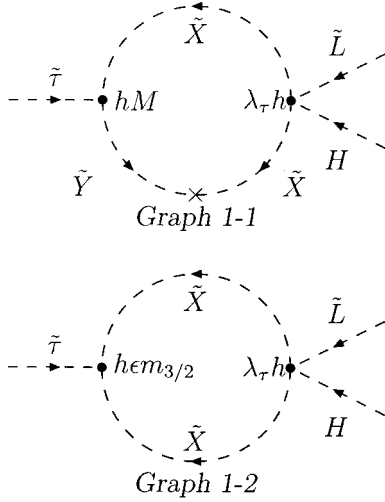
It is instructive to see the dependence on the momentum scale $\mu^2 = -k_\tau^2$. The sum of Graph 1-1 and Graph 1-2 is

$$i \frac{m_{3/2} h_0^* h_0 \lambda_{\tau,0}}{(4\pi)^2} \left\{ 1 - \frac{4M^2}{\mu \sqrt{\mu^2 + 4M^2}} \times \operatorname{arctanh} \frac{\mu}{\sqrt{\mu^2 + 4M^2}} \right\}, \quad (8.6)$$

which interpolates the result above threshold (8.4) and that below threshold (zero) as expected.

Graph 1-1 is finite by itself, so it is tempting to compute the threshold correction without using any regulator at all. And you do learn something when you do this: When you compute at scales $\mu \ll M$, you find the *negative* of the expected *above threshold* ($\mu \gg M$) anomaly-mediated contribu-

⁴To keep factors of (-1) and i straight, note that $i\mathcal{L} \ni -iA_{\tau LH} \tilde{\tau} \tilde{L} H$ and $i\mathcal{L} \ni (\text{Graph 1-2}) \tilde{\tau} \tilde{L} H$.

FIG. 1. Diagrams that contribute to the $A_{\tau LH}$ coupling.

tion to the A term. How do we interpret this result? This calculation computes the correct threshold correction, but to see the ultraviolet insensitivity, we should not ignore the piece it is correcting. A theory is only defined after specifying a regulator, be it Pauli-Villars, dimensional reduction, or what you will. Thus Graph 1-2 or its Pauli-Villars analogue always exists, regardless of how you treat the finite Graph 1-1. We must regulate, and when we include contributions from the regulator-induced operators, we find an A term which follows the trajectory defined by Eq. (8.1). The regulator diagram gives the contribution above threshold, and Graph 1-1 gives the threshold correction.

IX. SCALAR MASSES

As a final test of our formalism, we now compute the different above- and below-threshold anomaly-mediated contributions to the scalar masses. We recover the result of ultraviolet insensitivity, providing a resolution to the puzzle of Sec. III. To compare diagrammatic results with expressions for \tilde{m}_{τ}^2 , note that in the diagrams ‘‘Graph —’’ we compute are corrections to $i\mathcal{L}$, while $-i\tilde{m}_{\tau}^2\tilde{\tau}^*\tilde{\tau} \in i\mathcal{L}$.

A. Yukawa theory

1. Expectations

To understand our diagrammatic computation, we should first work out what we expect. We know that the scalar masses follow the form of Eq. (1.2),

$$\tilde{m}_{\tau}^2 = \frac{1}{2} m_{3/2}^2 \dot{\gamma}_{\tau}. \quad (9.1)$$

For easy comparison with the literature, we display $\dot{\gamma}_{\tau}$ in terms of renormalized couplings. However, we generally work in bare perturbation theory, and at two loops the renormalized and bare couplings differ significantly. In particular, when γ and $\dot{\gamma}$ are written in terms of the bare couplings, they contain additional scheme-dependent terms that vanish in the

limit that the cutoff, Λ , is taken to infinity (or $\epsilon \rightarrow 0$). Nevertheless, these additional terms are important during the regularized calculation, so we reexpress γ and $\dot{\gamma}$ in terms of bare couplings.

Working above threshold with the renormalized couplings,

$$\gamma_{\tau}(\mu) = \frac{1}{(4\pi)^2} [2\lambda_{\tau}^*(\mu)\lambda_{\tau}(\mu) + h^*(\mu)h(\mu)], \quad (9.2)$$

$$\gamma_{X_1}(\mu) = \gamma_{X_2}(\mu) = \frac{1}{(4\pi)^2} [h^*(\mu)h(\mu)], \quad (9.3)$$

$$\begin{aligned} \dot{\gamma}_{\tau}(\mu) &= \frac{1}{(4\pi)^2} [4\lambda_{\tau}(\mu)\lambda_{\tau}^*(\mu) + 2h(\mu)\dot{h}^*(\mu)] \\ &= \frac{1}{(4\pi)^2} [4\lambda_{\tau}^*(\mu)\lambda_{\tau}(\mu)(\gamma_{\tau} + \gamma_L + \gamma_H) \\ &\quad + 2h^*(\mu)h(\mu)(\gamma_{\tau} + \gamma_{X_1} + \gamma_{X_2})]. \end{aligned} \quad (9.4)$$

Below threshold the terms proportional to h^*h disappear, and in addition, γ_{τ} changes as from Eq. (8.2) to Eq. (8.3). Expanding to pinpoint the contributions to the scalar mass which change across the X and Y threshold, we find

$$\begin{aligned} \tilde{m}_{\tau}^2 &= \frac{m_{3/2}^2}{(4\pi)^4} [2\lambda_{\tau}^*\lambda_{\tau}(4\lambda_{\tau}^*\lambda_{\tau} + h^*h) \\ &\quad + h^*h(2\lambda_{\tau}^*\lambda_{\tau} + 3h^*h)] \quad (\text{above threshold}), \end{aligned} \quad (9.5)$$

$$\tilde{m}_{\tau}^2 = \frac{m_{3/2}^2}{(4\pi)^4} (8\lambda_{\tau}^*\lambda_{\tau}) \quad (\text{below threshold}). \quad (9.6)$$

Again, these expressions are written in terms of running couplings $\lambda_{\tau}(\mu)$, $h(\mu)$, and in keeping with our previously stated protocol, we now rewrite them in terms of bare couplings. By straightforward computation with DRED regularization, we can compute $\log Z$, from which it is straightforward to extract \tilde{m}_{τ} .⁵ We find

$$\begin{aligned} \tilde{m}_{\tau}^2 &= \frac{m_{3/2}^2}{(4\pi)^2} \left\{ -2 \frac{\epsilon\lambda_{\tau,0}^*\lambda_{\tau,0}}{(\mu^2)^{\epsilon}} - \frac{\epsilon h_0^*h_0}{(\mu^2)^{\epsilon}} + \frac{1}{(4\pi)^2} \left(16 \frac{(\lambda_{\tau,0}^*\lambda_{\tau,0})^2}{(\mu^2)^{2\epsilon}} \right. \right. \\ &\quad \left. \left. + 6 \frac{(h_0^*h_0)^2}{(\mu^2)^{2\epsilon}} + 8 \frac{\lambda_{\tau,0}^*\lambda_{\tau,0}h_0^*h_0}{(\mu^2)^{2\epsilon}} \right) \right\} \\ & \quad (\text{above threshold, bare couplings}). \end{aligned} \quad (9.7)$$

⁵As an alternative to direct computation, we can find $\dot{\gamma}_{\tau}$, and hence \tilde{m}_{τ}^2 , through renormalization group arguments. This method is explicitly implemented for the gauge theory in Appendix C.

Below threshold, terms in Z_τ proportional to $h_0^* h_0 / (\mu^2)^\epsilon$ are modified to $h_0^* h_0 / (M^2)^\epsilon$, because X fluctuations are cut off at scales $\mu \ll M$. This means that most of the h dependence drops out of $\dot{\gamma}_\tau$, as in Eq. (9.6). Here, however, a $\lambda_{\tau,0}^* \lambda_{\tau,0} h_0^* h_0$ term remains:

$$\begin{aligned} \tilde{m}_\tau^2 = & \frac{m_{3/2}^2}{(4\pi)^2} \left\{ -2 \frac{\epsilon \lambda_{\tau,0}^* \lambda_{\tau,0}}{(\mu^2)^\epsilon} + \frac{1}{(4\pi)^2} \left(16 \frac{(\lambda_{\tau,0}^* \lambda_{\tau,0})^2}{(\mu^2)^{2\epsilon}} \right. \right. \\ & \left. \left. + 2 \frac{\lambda_{\tau,0}^* \lambda_{\tau,0} h_0^* h_0}{(\mu^2)^\epsilon (M^2)^\epsilon} \right) \right\} \\ & \text{(below threshold, bare couplings).} \end{aligned} \quad (9.8)$$

The residual h_0 dependence below threshold just reflects our use of bare couplings. Of course the heavy particles decouple from the physics at scales $\mu \ll M$, and we see this when we use renormalized couplings as in Eq. (9.6). As an aside, we mention that there is a factor of two difference between terms that go like the fourth power of the coupling constant when we compare Eqs. (9.8) and (9.6). The reason is that in Eq. (9.8), part of the $(\lambda_{\tau,0}^* \lambda_{\tau,0})^2$ term combines with the $\mathcal{O}(\epsilon)$ piece to give a piece that vanishes in the four-dimensional limit.

2. One-loop contributions

We now turn to the calculation of the diagrams. As mentioned previously, for simplicity we compute below-threshold contributions to \tilde{m}_τ^2 at zero external momentum. Above threshold we neglect the X and Y mass M relative to a finite external momentum. This procedure, together with the mass insertion formalism, means that in any given diagram there is only one fixed mass/momentum scale, a tremendous advantage computationally. Further, when $M \rightarrow 0$, there are fewer vertices and consequently many fewer diagrams.

As seen in Eqs. (9.7) and (9.8), when we write the scalar mass in terms of bare couplings there is a one-loop $\mathcal{O}(\epsilon)$ piece. These one-loop $\mathcal{O}(\epsilon)$ terms occur diagrammatically as shown in Fig. 2. Above the X - Y mass threshold we can take $M \rightarrow 0$, so Graphs 2-3, 2-4, and 2-5 all vanish, as they contain vertices hM and/or $Mm_{3/2}$. This leaves Graph 2-1 and Graph 2-2. Poles from the logarithmically divergent loop integrals pair with the $\mathcal{O}(\epsilon^2)$ contribution from the vertices to give $\mathcal{O}(\epsilon)$ results:

$$\text{Graph 2-1} = i\epsilon h_0^* h_0 \frac{m_{3/2}^2}{(4\pi)^2 (\mu^2)^\epsilon} \quad (9.9)$$

$$\text{Graph 2-2} = 2i\epsilon \lambda_{\tau,0}^* \lambda_{\tau,0} \frac{m_{3/2}^2}{(4\pi)^2 (\mu^2)^\epsilon}, \quad (9.10)$$

matching our expectations from Eq. (9.7). Below threshold, Graph 2-1 comes with $(\mu^2)^\epsilon$ replaced by $(M^2)^\epsilon$, while Graph 2-3, Graph 2-4 and Graph 2-5 sum to give

Graph 2-3 + Graph 2-4 + Graph 2-5

$$= -i\epsilon h_0^* h_0 \frac{m_{3/2}^2}{(4\pi)^2 (M^2)^\epsilon}, \quad (9.11)$$

canceling the $h_0^* h_0$ dependence of Eq. (9.7) as required by Eq. (9.8). Other one-loop graphs potentially contributing finite terms to the scalar mass cancel among themselves.

3. $\lambda_{\tau,0}^* \lambda_{\tau,0} h_0^* h_0$ contributions

There are two types of $\lambda_\tau^2 h^2$ contributions to the scalar mass. The straightforward two-loop diagrams appear in Fig. 3. Only Graph 3-2 exists above threshold:

$$\text{Graph 3-2} = -4i\lambda_{\tau,0}^* \lambda_{\tau,0} h_0^* h_0 \frac{m_{3/2}^2}{(4\pi)^4 (\mu^2)^{2\epsilon}}. \quad (9.12)$$

This is half of the $\lambda_{\tau,0}^* \lambda_{\tau,0} h_0^* h_0$ dependence needed for \tilde{m}_τ^2 in Eq. (9.7). As expected, it is the diagram containing vertices proportional to ϵ which yields the contribution to the anomaly-mediated scalar mass.

The other above-threshold contribution comes from the cross term between the wave-function renormalization and the $\mathcal{O}(\epsilon)$ one-loop scalar mass derived in Sec. IX A 2. Since the anomaly mediated soft scalar mass [Eq. (1.2) or (9.7)] is the mass in a canonically normalized Lagrangian, we need to divide the mass-renormalization part of our two-point function by the wave-function-renormalization part, $Z_\tau = 1 + \delta Z_\tau$, when computing corrections to the mass squared. Cross terms between δZ_τ and two-loop mass diagrams are higher order, but cross terms between δZ_τ and the one-loop mass diagrams contribute at $\mathcal{O}(\lambda_\tau^2 h^2)$.

Since δZ_τ will multiply the $\mathcal{O}(\epsilon)$ one-loop masses, we only need the $\mathcal{O}(1/\epsilon)$ poles (see Fig. 4). With external momentum p ,

$$\text{Graph 4-1} = i h_0^* h_0 \frac{p^2}{(4\pi)^2 (-p^2)^\epsilon} \frac{1}{\epsilon} + \mathcal{O}(\epsilon^0) \quad (9.13)$$

$$\text{Graph 4-2} = 2i\lambda_{\tau,0}^* \lambda_{\tau,0} \frac{p^2}{(4\pi)^2 (-p^2)^\epsilon} \frac{1}{\epsilon} + \mathcal{O}(\epsilon^0), \quad (9.14)$$

which means

$$\delta Z_\tau = \frac{h_0^* h_0 + 2\lambda_{\tau,0}^* \lambda_{\tau,0}}{(4\pi)^2 (\mu^2)^\epsilon} \frac{1}{\epsilon} + \mathcal{O}(\epsilon^0). \quad (9.15)$$

To lowest order, dividing by $Z_\tau = 1 + \delta Z_\tau$ means multiplying by $(1 - \delta Z_\tau)$, so our sought-after contribution is

$$\begin{aligned} & -\delta Z_\tau \times (\text{Graph 2-1} + \text{Graph 2-2}) \\ & = [-2i\lambda_{\tau,0}^* \lambda_{\tau,0} h^2 - 2i\lambda_{\tau,0}^* \lambda_{\tau,0} h_0^* h_0 - i(h_0^* h_0)^2 \\ & \quad - 4i(\lambda_{\tau,0}^* \lambda_{\tau,0})^2] \frac{m_{3/2}^2}{(4\pi)^4 (\mu^2)^{2\epsilon}}. \end{aligned} \quad (9.16)$$

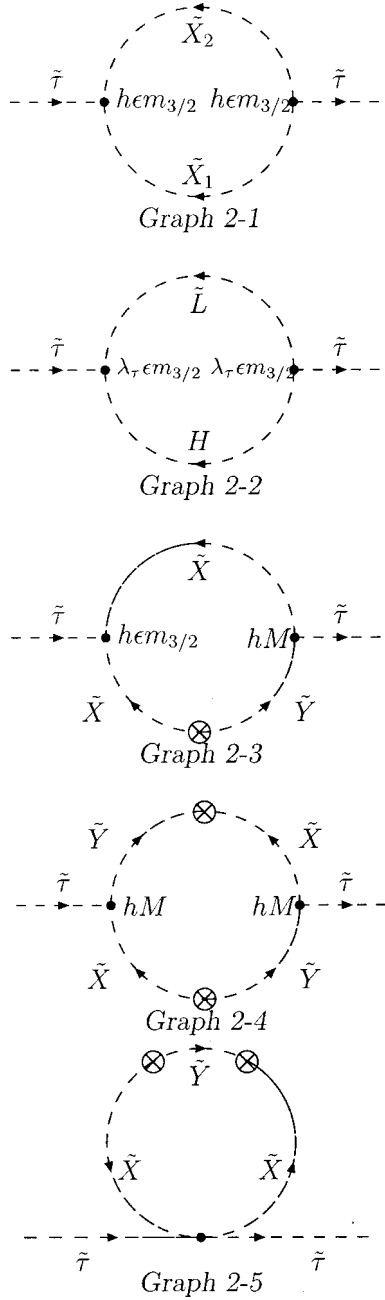


FIG. 2. Diagrams contributing the one-loop $\mathcal{O}(\epsilon)$ terms to the scalar mass squared.

These two $2\lambda_{\tau,0}^*\lambda_{\tau,0}h_0^*h_0$ pieces combine with the $4\lambda_{\tau,0}^*\lambda_{\tau,0}h_0^*h_0$ piece from Eq. (9.12) to exhaust the $8\lambda_{\tau,0}^*\lambda_{\tau,0}h_0^*h_0$ of Eq. (9.7).

Below threshold the cancellation of much of the $\lambda_{\tau,0}^*\lambda_{\tau,0}h_0^*h_0$ dependence proceeds as follows: we find Graph 3-1 supplies a threshold correction

$$\text{Graph 3-1} = 4ih_0^*h_0\lambda_{\tau,0}^*\lambda_{\tau,0}\frac{m_{3/2}^2}{(4\pi)^4(\mu^2)^\epsilon(M^2)^\epsilon}, \quad (9.17)$$

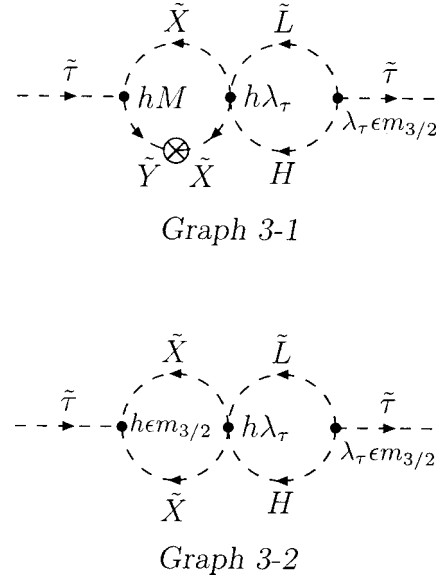


FIG. 3. Diagrams that contribute $\lambda_{\tau,0}^*\lambda_{\tau,0}h_0^*h_0$ terms to the scalar mass.

which exactly cancels Graph 3-2 in Eq. (9.12) after the replacement $(\mu^2)^{2\epsilon} \rightarrow (\mu^2)^\epsilon(M^2)^\epsilon$. We already discussed in Sec. IX A 2 how Graphs 2-3, 2-4, and 2-5 cancel Graph 2-1 below threshold. This leaves the cross term between δZ_τ and Graph 2-2, one of the terms from Eq. (9.16). Below threshold the $h_0^*h_0(\mu^2)^{-\epsilon}$ dependence in δZ_τ becomes $h_0^*h_0(M^2)^{-\epsilon}$, so that the cross term becomes

$$-\delta Z_\tau \times (\text{Graph 2-2}) \ni -2i\lambda_{\tau,0}^*\lambda_{\tau,0}h_0^*h_0\frac{m_{3/2}^2}{(4\pi)^4(\mu^2)^\epsilon(M^2)^\epsilon}, \quad (9.18)$$

which is the residual $\lambda_{\tau,0}^*\lambda_{\tau,0}h_0^*h_0$ dependence in Eq. (9.8). This confirms the ultraviolet insensitivity: We have checked Eq. (9.8), and when we rewrite that equation in terms of renormalized couplings, we find Eq. (9.6). There the ultraviolet insensitivity is manifest.

4. $(h_0^*h_0)^2$ contributions

For now we continue to work exclusively with bare couplings; the relevant \tilde{m}_τ^2 for comparison is that of Eqs. (9.7) and (9.8). The new $(h_0^*h_0)^2$ diagrams appear in Figs. 5 and 6. The graphs shown are merely skeletons, the true diagrams being found by adding mass insertions and the various trilinear couplings in all possible places.

We first proceed with the calculation of the anomaly mediated contribution to the scalar mass above threshold. We expect our result to agree with the $(h_0^*h_0)^2$ term in Eq. (9.7). Of the graphs in the figure, only some occur above threshold—Graphs 5-3, 5-5, 5-7, and 6-2, each with two trilinear vertices $h_0\epsilon m_{3/2}\tilde{\tau}\tilde{X}_1\tilde{X}_2$. The others vanish in the $M \rightarrow 0$ limit.

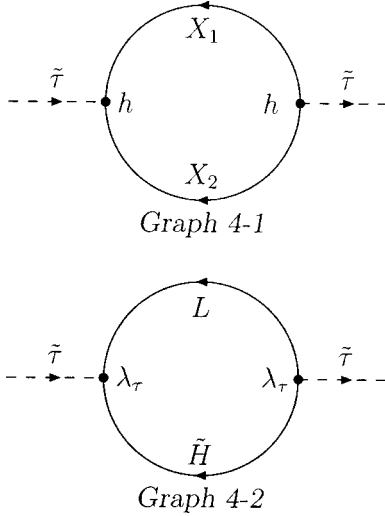


FIG. 4. Diagrams for the one-loop $O(1/\epsilon)$ wave-function renormalization.

The calculations are straightforward except for Graph 5-5. This diagram is different from the others in that it has an infrared divergence in the lower loop which is not regulated by the external momentum. However, the top loop is effectively a contribution to the \tilde{X} two-point function, and if we integrate that loop first, it gives a radiatively-generated mass to the \tilde{X} boson which regulates the infrared divergence. (Recall that we are working in the limit where the tree mass $M \rightarrow 0$. The vertices which appear in computing the one-loop \tilde{X} two-point function are $h_0 \epsilon m_{3/2} \tilde{\tau} \tilde{X}_1 \tilde{X}_2$ and its Hermitian conjugate.) We will have more to say about infrared divergences in dimensional reduction when we discuss the gauge theory.

The values of the above-threshold diagrams appear in Table I. Also included is the $(h_0^* h_0)^2$ contribution derived in Eq. (9.16), which comes from the cross term between the one-loop $O(\epsilon)$ scalar mass and the wave-function renormalization. Altogether, we find the expected above-threshold result

$$\tilde{m}_\tau^2 \ni 6(h_0^* h_0)^2 \frac{m_{3/2}^2}{(4\pi)^4 (\mu^2)^{2\epsilon}}. \quad (9.19)$$

We now turn to the calculation of the $(h_0^* h_0)^2$ piece of the τ -scalar mass below threshold. Based on Eq. (9.8), we expect to find zero. Below threshold, the cross-term between the one-loop $O(\epsilon)$ mass and the wave-function renormalization disappears because the sum of Graphs 2-3, 2-4, and 2-5 cancels Graph 2-1. Then we are left with two-loop diagrams from Figs. 5 and 6, all of which contribute below threshold. We split our computation into three parts. First, there are diagrams in which all trilinear vertices are of the form $h_0 M \tilde{\tau} \tilde{X} \tilde{Y}$, and supersymmetry-breaking comes from a pair of mass insertions $M m_{3/2}$ on the scalar lines. Second, there are diagrams with a single ϵ trilinear vertex and a single $M m_{3/2}$ insertion. Finally, there are the same diagrams which existed above threshold, where two trilinear vertices are of

TABLE I. Values [to $O(\epsilon^0)$] of the diagrams suppling the above-threshold $(h_0^* h_0)^2$ term in the scalar mass squared. We have pulled out a common factor $[1/(4\pi)^4] i (h_0^* h_0)^2 m_{3/2}^2 (\mu^2)^{-2\epsilon}$.

Graph 5-3	-2
Graph 5-5	-1
Graph 5-7	-1
Graph 6-2	-1
Equation (9.16)	-1

the form $h_0 \epsilon m_{3/2} \tilde{\tau} \tilde{X}_1 \tilde{X}_2$. Using the integrals $I(m, n, l)$, $F(m, n, l)$, and $G(m, n, l)$ as defined in Appendix A, we write down the values for the Feynman diagrams in a compact form in Table II.

Expanding the integrals and summing all contributions, we find exact cancellation, matching Eq. (9.8) and verifying ultraviolet insensitivity. In particular, the cancellation among the $O(\epsilon^0)$ terms looks like

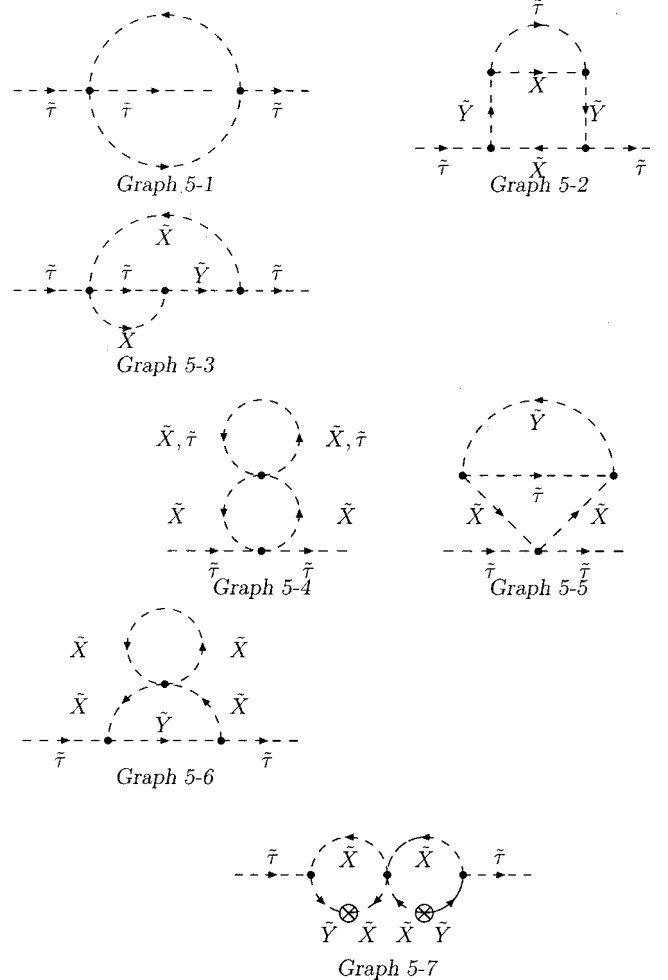


FIG. 5. Diagrams that contribute to the h^4 threshold correction that exclusively include scalars. These diagrams may be defined in terms of the integral $I(m, n, l)$ as defined in the text. Where \tilde{X} is shown, it corresponds to both \tilde{X}_1 and \tilde{X}_2 , as appropriate. Also, the three point scalar couplings shown here are the vertices $hM \tilde{\tau} \tilde{X} \tilde{Y}^*$. As described in the text, this vertex can be replaced with the $\epsilon \tilde{\tau} \tilde{X} \tilde{X}$ vertex, yielding additional diagrams.

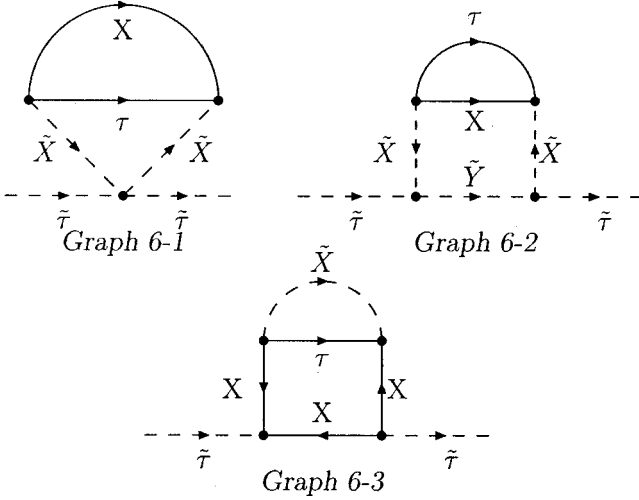


FIG. 6. Diagrams that contribute to the h^4 threshold correction that include fermions.

$$0 = i(h_0^* h_0)^2 \frac{m_{3/2}^2}{(4\pi)^4 (M^2)^{2\epsilon}} (-5 + 10 - 5) \quad (9.20)$$

where the contributions are, respectively, from graphs with zero, one, or two $h_0 \epsilon m_{3/2} \tilde{\tau} \tilde{X}_1 \tilde{X}_2$ vertices. [Table VII gives $\mathcal{O}(\epsilon^0)$ expansions for the integrals, but the spurion computation assures us that the cancellation is exact, and it does indeed extend to all orders in ϵ .]

Now it is instructive to revisit our puzzle of Sec. III. When we found a vanishing threshold correction and a resulting lack of ultraviolet insensitivity, it was because we had not calculated all contributions to the scalar mass. In the language of this section, we calculated the first section of Table II, along with a cross-term from Graph 4-1 and Graphs 2-4 and 2-5. We then added in a contribution from the A -term by hand. This gave an erroneous result. We have seen that the correct procedure is to calculate the entirety of Table II, and see that the contributions sum to zero.

5. Finite computation for $(h^* h)^2$

In contrast to the DRED calculation above, we present an additional calculation that does not depend on this type of regularization. In the language of Sec. III, this calculation corresponds to one where we have implicitly used a holomorphic regularization scheme. So, we may compare this calculation to the spurion calculation done with holomorphic regularization. This provides an additional demonstration of the ultraviolet insensitivity.

As described in Sec. III, we must keep all integrals in four dimensions, paying attention to the finiteness of the integrals. By integrating out the cut-off dependent supersymmetry-breaking operators, we recover the anomaly mediated piece of Eq. (1.2). If we choose Pauli-Villars as our holomorphic regulator, this procedure would essentially correspond to working with an effective Lagrangian at a scale μ below the threshold of the Pauli-Villars particles. We have integrated out the Pauli-Villars fields, and the anomaly-mediated soft terms now appear in our effective Lagrangian. Keeping this

TABLE II. Below-threshold contributions to $(h_0^* h_0)^2$ terms in the scalar mass squared. The three sets of values represent diagrams in which zero, one, or two trilinear vertices are of the form $h_0 \epsilon m_{3/2} \tau X_1 X_2$. The integrals $I(m, n, l)$, $F(m, n, l)$, and $G(m, n, l)$ are defined in Appendix A. We have pulled out a common factor $i(h_0^* h_0)^2 m_{3/2}^2$.

Graph 5-1	$4M^2 I(3,1,1)$
Graph 5-2	$24M^6 I(5,1,1) + 12M^6 I(4,2,1) + 4M^6 I(3,3,1)$
Graph 5-3	$12M^4 I(3,2,1) + 12M^4 I(4,1,1)$
Graph 5-4	$4M^2 I(4,1,0) + 2M^2 I(3,2,0)$
Graph 5-5	$6M^4 I(3,2,1) + 6M^4 I(4,1,1)$
Graph 5-6	$2M^4 I(3,3,0) + 12M^4 I(5,1,0)$
Graph 5-7	$4M^4 I(3,3,0)$
Graph 6-1	$-8M^2 F(4,1,1)$
Graph 6-2	$-24M^4 F(5,1,1)$
Graph 6-3	$4M^6 G(3,3,1)$
Graph 5-2	$24\epsilon M^4 I(4,1,1) + 8\epsilon M^4 I(3,2,1)$
Graph 5-3	$12\epsilon M^2 I(3,1,1) + 4\epsilon M^2 I(2,2,1)$
Graph 5-5	$4\epsilon M^2 I(2,2,1) + 4\epsilon M^2 I(3,1,1)$
Graph 5-6	$8\epsilon M^2 I(4,1,0)$
Graph 5-7	$4\epsilon M^2 I(3,2,0)$
Graph 6-2	$-16\epsilon M^2 F(4,1,1)$
Graph 5-2	$8\epsilon^2 I(3,1,1)$
Graph 5-3	$4\epsilon^2 I(2,1,1)$
Graph 5-5	$2\epsilon^2 I(2,1,1)$
Graph 5-6	$2\epsilon^2 I(3,1,0)$
Graph 5-7	$\epsilon^2 I(2,2,0)$
Graph 6-2	$-4\epsilon^2 F(3,1,1)$

anomaly-mediated piece in mind, we may turn to a calculation of the threshold correction. We calculate the diagrams with \tilde{X} and \tilde{Y} particles in the loops, taking care to keep our integrals well defined at all times.

First, the A terms in the effective Lagrangian give rise to the diagram in Fig. 7. This is effectively a two-loop diagram because there is one-loop suppression through the A term. It is already finite. Recalling that $A_{\tau X_1 X_2} = -m_{3/2} h (\gamma_\tau + \gamma_{X_1} + \gamma_{X_2})$,

$$\begin{aligned} \text{Graph 7-1} &= 2ih^* h \frac{m_{3/2}^2}{(4\pi)^2} (\gamma_\tau + \gamma_{X_1} + \gamma_{X_2}) \\ &= 2ih^* h \frac{m_{3/2}^2}{(4\pi)^4} (2\lambda_\tau^* \lambda_\tau + 3h^* h). \end{aligned} \quad (9.21)$$

The remaining relevant diagrams and their formal values appear in the first part of Table II. Of these only a few are potentially divergent. Expanding $F(l, m, n)$ and $G(l, m, n)$ in terms of $I(l, m, n)$, we find

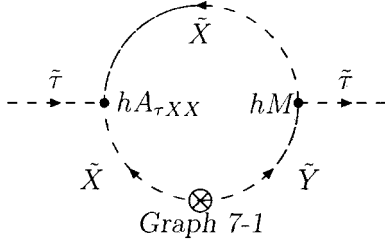


FIG. 7. Additional diagram for the finite h^4 calculation. It is effectively a two-loop diagram, as there is a one-loop suppression through the A -term vertex.

$$\begin{aligned} \text{Sum of diagrams} = & \text{finite} + [24M^6 I(5,1,1) \\ & + 30M^4 I(4,1,1) + 6M^2 I(3,1,1)]. \end{aligned} \quad (9.22)$$

The last three terms are individually divergent, but their sum is clearly not, since the left-hand side is finite. In Appendix B we outline a completely finite calculation of these terms. All told, we find that the finite evaluation of these diagrams yields precisely $-3i(h^*h)^2[1/(4\pi)^4]m_{3/2}^2$. When added with the $6i(h^*h)^2[1/(4\pi)^4]m_{3/2}^2$ contribution from Eq. (9.21), we find a total $3i(h^*h)^2[1/(4\pi)^4]m_{3/2}^2$. This is the proper threshold correction to cancel the known above-threshold contribution from the Pauli-Villars fields as given in terms of renormalized couplings, Eq. (9.5). This again verifies ultraviolet insensitivity.

It is worth contrasting how the cancellation happens in dimensional reduction [Eq. (9.20)]. In that case the diagrams with no ϵ -dependent vertices contribute $-5(h_0^*h_0)^2$, versus $-3(h^*h)^2$ in the completely finite calculation. This is a signal that we must include the ϵ -dependent vertices to get the consistent results. The dimensional reduction cancellation happens through complicated interplay between these diagrams and those with the new ϵ vertices.

Finally, we mention that the couplings throughout our “finite calculation” are the renormalized couplings, $h(\mu)$. This is because we have generated the soft terms by integrating out the Pauli-Villars fields at the cutoff scale to get Eqs. (1.1) and (1.2). However, these equations are renormalization group invariant, so, we can run them down to our threshold scale M where the equations still hold, now evaluated at the renormalization group (RG) scale M . This threshold correction is then done with couplings at this scale, in other words, with the renormalized couplings.

6. $(\lambda_{\tau,0}^* \lambda_{\tau,0})^2$ contributions

The calculation of $(\lambda_{\tau,0}^* \lambda_{\tau,0})^2$ contributions to \tilde{m}_τ^2 is identical to the above-threshold $(h_0^*h_0)^2$ calculation, the only difference being factors of two from the doublets L and H . The table analogous to Table I is Table III. Summing, we find the $16(\lambda_{\tau,0}^* \lambda_{\tau,0})^2$ expected in Eq. (9.7). $(\lambda_{\tau,0}^* \lambda_{\tau,0})^2$ contributions are not affected by integrating out the heavy X and Y fields.

In summary, we have utilized our new formalism in DRED to check two anomaly-mediated calculations. First of

all, we were able to check the usual form of the anomaly mediated contributions to A terms and scalar masses. Second, we were able to explicitly verify the ultraviolet insensitivity of anomaly mediation through a diagrammatic calculation.

B. Abelian gauge theory

1. Expectations

Shifting to the U(1) gauge model described in Sec. VII, we have particle content τ, X_1, Y_1, X_2, Y_2 , with superpotential given in Eq. (7.2). In this section we primarily focus on additional subtleties that arise for the gauge theory. We show a computation of the above-threshold anomaly-mediated contributions proportional to Y_τ^2 and $Y_\tau^2 Y_X^2$. We further check that the contributions going like $Y_\tau^2 Y_X^2$ vanish below threshold, confirming ultraviolet insensitivity. We believe these calculations capture the subtleties associated with the gauge theory. Incidentally, the calculation of the anomaly-mediated contributions in this model is quite similar to a gauge mediation calculation performed previously [16].

Before calculating any diagrams, it is important to know what we expect for the scalar mass. For this, we need to know $\dot{\gamma}$. It is useful to write the results in terms of both renormalized and bare couplings. In terms of renormalized couplings we have

$$\gamma_\tau(\mu) = \frac{1}{(4\pi)^2} [-2g'^2(\mu) Y_\tau^2], \quad (9.23)$$

$$\begin{aligned} \dot{\gamma}_\tau(\mu) &= \frac{1}{(4\pi)^2} [-4g'(\mu)\dot{g}'(\mu) Y_\tau^2] \\ &= \frac{1}{(4\pi)^4} [-4g'^4(\mu) Y_\tau^2 (Y_\tau^2 + Y_{X_1}^2 + Y_{Y_1}^2 + Y_{X_2}^2 + Y_{Y_2}^2)] \\ &= \frac{1}{(4\pi)^4} \left[-4g'^4(\mu) Y_\tau^2 \left(Y_\tau^2 + \sum_{\text{heavy}} Y_i^2 \right) \right]. \end{aligned} \quad (9.24)$$

(Here and below, the sum over heavy multiplets is performed for each chiral superfield separately.) Then clearly,

$$\begin{aligned} \tilde{m}_\tau^2 &= \frac{m_{3/2}^2}{(4\pi)^4} \left[-2g'^4(\mu) Y_\tau^2 \left(Y_\tau^2 + \sum_{\text{heavy}} Y_i^2 \right) \right] \\ & \quad (\text{above threshold}), \end{aligned} \quad (9.25)$$

$$\tilde{m}_\tau^2 = \frac{m_{3/2}^2}{(4\pi)^4} [-2g'^4(\mu) Y_\tau^4] \quad (\text{below threshold}). \quad (9.26)$$

The last expression does not depend on the properties of heavy particles at all, manifesting the UV insensitivity. To

TABLE III. Values [to $O(\epsilon^0)$] of the diagrams suppling above-threshold $(\lambda_{\tau,0}^* \lambda_{\tau,0})^2$ term in the scalar mass squared. We have pulled out a common factor $i(\lambda_{\tau,0}^* \lambda_{\tau,0})^2 [1/(4\pi)^4] m_{3/2}^2 (\mu^2)^{-2\epsilon}$. Everywhere in Graphs 5-2 through 6-2 L and H replace X and Y .

Graph 5-2	0
Graph 5-3	-4
Graph 5-5	-2
Graph 5-7	-4
Graph 6-2	-2
Equation (9.16)	-4

get the analogous expressions in terms of the bare couplings requires a bit more work. This calculation is done in Appendix C. In terms of bare couplings we have

$$\tilde{m}_\tau^2 = \frac{m_{3/2}^2}{(4\pi)^2} \left(2 \frac{\epsilon Y_\tau^2 g_0'^2}{(\mu^2)^\epsilon} - 4 \frac{g_0'^4 Y_\tau^2 \left(Y_\tau^2 + \sum_{\text{heavy}} Y_i^2 \right)}{(4\pi)^2 (\mu^2)^{2\epsilon}} \right)$$

(above threshold, bare couplings), (9.27)

$$\tilde{m}_\tau^2 = \frac{m_{3/2}^2}{(4\pi)^2} \left(2 \frac{\epsilon Y_\tau^2 g_0'^2}{(\mu^2)^\epsilon} - 4 \frac{g_0'^4 Y_\tau^4}{(4\pi)^2 (\mu^2)^{2\epsilon}} - 2 \frac{g_0'^4 Y_\tau^2 \sum_{\text{heavy}} Y_i^2}{(4\pi)^2 (\mu^2)^\epsilon (M^2)^\epsilon} \right)$$

(below threshold, bare couplings). (9.28)

2. Insensitivity

In this section we will compute the above-threshold anomaly-mediated contributions proportional to Y_τ^2 and $Y_\tau^2 Y_{X_i}^2$, and we check that the latter vanish below threshold to confirm ultraviolet sensitivity. The relevant skeleton diagrams are shown in Fig. 8; we must add appropriate supersymmetry-breaking vertices to form the actual diagrams. (There are many additional diagrams which give Y_τ^4 contributions, but we do not expect further conceptual difficulties in their calculation.)

Let us consider the contribution to the scalar masses above threshold. In this energy regime the SUSY-breaking $M m_{3/2}$ mass insertion is suppressed ($M \rightarrow 0$), so there are only two sources of supersymmetry breaking. First there is a tree-level gaugino mass, $m_\lambda = -\epsilon m_{3/2}$. Then depending on the choice of the bare Lagrangian, Eq. (4.13) or Eq. (4.10), the remaining supersymmetry breaking is given by the non-local gaugino operator in Eq. (4.14) or by the ϵ -scalar mass, $m_\epsilon = \epsilon m_{3/2}^2$, that results from using the GMZ operator.

The diagrams in Fig. 9 yield the one-loop $\mathcal{O}(\epsilon)$ piece in Eqs. (9.27) and (9.28). Depending on our form for the bare Lagrangian, either Graph 9-1 or Graph 9-2 contributes. The

values of the diagrams appear in Table IV.

The two-loop terms come from one or two diagrams. If we choose to work with the non-local operator, only gauginos have supersymmetry breaking, and so only the single topology Graph 8-6 contributes. If instead we work with a supersymmetry-breaking mass for the epsilon scalar, Graph 10-1 (see Fig. 10) adds to a reduced contribution from Graph 8-6. Table V collects these contributions to the scalar mass, which total

$$\tilde{m}_\tau^2 \ni -4 g_0'^4 Y_\tau^2 \sum_{\text{heavy}} Y_i^2 \frac{m_{3/2}^2}{(4\pi)^4 (\mu^2)^{2\epsilon}}. \quad (9.29)$$

This completes the calculation of the mass above the threshold. We now demonstrate decoupling. All graphs in Fig. 8 are relevant, because below threshold we keep a finite X - Y mass M , and supersymmetry breaking enters through an $\tilde{X}\tilde{Y}$ mass insertion. First we consider only the diagrams with this sort of supersymmetry breaking. There appear to be seven such diagrams, but several of these in fact do not contribute.

Graph 8-5 vanishes because it is proportional to the sum of the flavor charges of the heavy fields. This sum vanishes by the gauge invariance of the Lagrangian. The sum of Graph 8-2 and Graph 8-4 also vanishes by gauge invariance: If we add Graph 8-4 and Graph 8-2, we get a graph that contains the vacuum polarization operator for scalar QED, with a form fixed by gauge invariance to be

$$\Pi^{\mu\nu} = (p^\mu p^\nu - p^2 g^{\mu\nu}) \Pi(p^2). \quad (9.30)$$

Upon contraction with the momentum-dependent $(\tilde{\tau} \partial_\mu \tilde{\tau}^* A^\mu + \text{H.c.})$ vertex, the sum of Graphs 8-2 and 8-4 yields zero. Thus only four graphs containing supersymmetry breaking due to the $M m_{3/2}$ mass insertion contribute to the threshold correction: Graphs 8-3, 8-6, and the combination of Graph 8-1 and Graph 8-7 which again contains the vacuum polarization operator.

There is a remaining worry concerning infrared divergences. We can safely express Graph 8-3 in terms of the standard integrals in Appendix A, but we must be more careful with the other graphs. If blithely written in terms of $I(m, n, l)$, the diagrams contain infrared-divergent integrals which are not automatically regulated by DRED. While in DREG one can analytically continue to $4 + 2\epsilon$ dimensions to regulate the IR, DRED by definition *compactifies* 4 dimensions down to $4 - 2\epsilon$ dimensions. IR-divergent integrals are thus not well defined by DRED, and one can find mutually inconsistent ways to evaluate such integrals. In particular, the sometimes-seen prescription

$$\int \frac{d^4 p}{p^4} = 0 \quad (\text{inconsistent}) \quad (9.31)$$

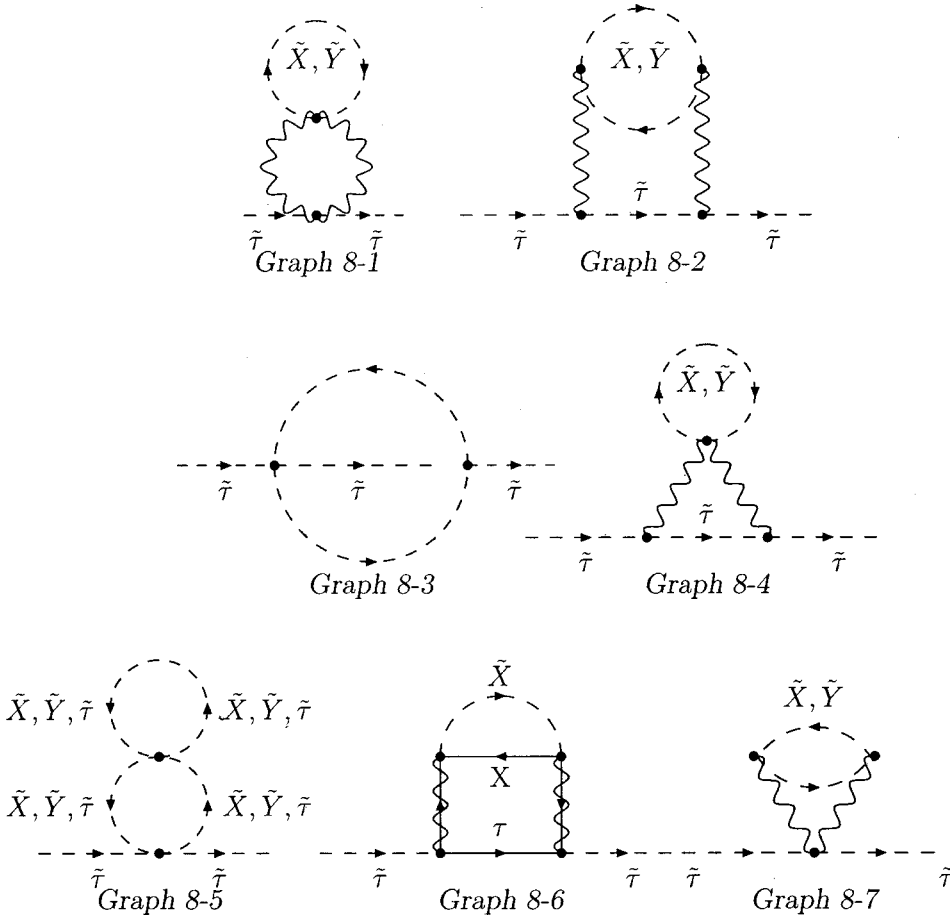


FIG. 8. Diagrams that contribute to the cancellation in g'^4 . These diagrams all contain the heavy fields \tilde{X} and \tilde{Y} .

leads to inconsistent results. Nonetheless, in supersymmetry we must use DRED, and not DREG, because an extension above 4 dimensions changes the spinor algebra and causes a mismatch in the fermionic and boson degrees of freedom. In short, a safe and consistent procedure is to use DRED to regulate the UV and add finite masses to regulate the IR when necessary.

Fortunately in our case, we can largely avoid the infrared divergences. There are only two cases where we find IR divergences to be an issue. The first is Graph 8-1 where the ϵ -scalar replaces the vector boson. The second is in Graph 8-6 when there is supersymmetry breaking from the non-local contribution to the gaugino propagator. In these cases, we keep a finite mass. Among the other graphs, once Graph 8-1 and Graph 8-7 are combined, the sum is manifestly infrared finite. Graph 8-6 (without the non-local term in the gaugino propagator) and Graph 8-3 are each infrared finite on their own. We evaluate these two graphs directly, and their result is shown in Table VI.

We evaluate Graph 8-1 and Graph 8-7 by summing their top loops into the vacuum polarization operator and then contracting this subgraph with the seagull vertex. This avoids all ambiguities due to infrared divergences. To compute the explicit form of the vacuum polarization operator, we found it easier to work in the mass eigenbasis, where the scalars have masses $M^2 \pm Mm_{3/2}$, and then to expand to $O(m_{3/2}^2)$. For a scalar particle of mass M and charge Y_X (in the mass eigenbasis),

$$\begin{aligned} \Pi(p^2) &= (p^\mu p^\nu - p^2 g^{\mu\nu}) \frac{-Y_X^2 g_0'^2 i\Gamma(\epsilon)}{(4\pi)^{2-\epsilon}} \\ &\times \int_0^1 dx \frac{(1-2x)^2}{[M^2 - p^2 x(1-x)]^\epsilon}. \end{aligned} \quad (9.32)$$

Summing over the two eigenmasses and expanding in $m_{3/2}$, we find the vacuum polarization in the mass insertion formalism:

$$\begin{aligned} \Pi(p^2) &= (p^\mu p^\nu - p^2 g^{\mu\nu}) (im_{3/2}^2 M^2) \frac{Y_X^2 g_0'^2 \Gamma(2+\epsilon)}{(4\pi)^{2-\epsilon}} \\ &\times \int_0^1 dx \frac{(1-2x)^2}{[M^2 - p^2(1-x)x]^{2+\epsilon}}. \end{aligned} \quad (9.33)$$

We contract this result with the seagull vertex to obtain a final value for Graphs 8-1 and 8-7. The result appears in Table VI.

There are further contributions in which supersymmetry breaking does not come from the B-type mass. The tree-level gaugino mass equal to $-\epsilon m_{3/2}$ enters a diagram identical to Graph 8-6, but with one or both of the $\tilde{X}\tilde{Y}$ mass insertions replaced by gaugino mass insertions. Finally, there are the diagrams involving either the non-local correction to the gaugino propagator [Eq. (4.14)] or a massive ϵ scalar [Eq.

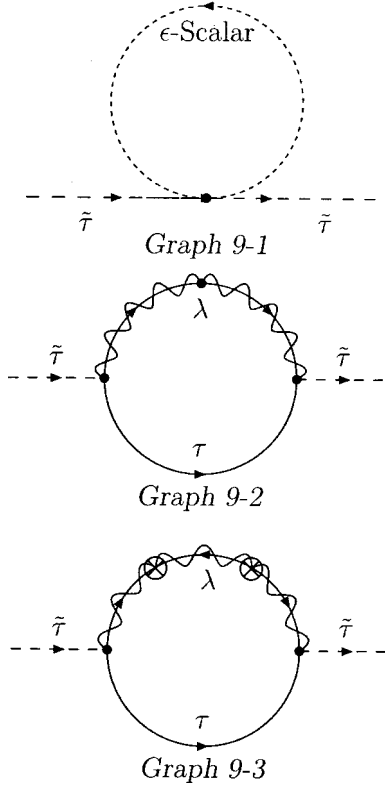


FIG. 9. Diagrams that contribute to the $\mathcal{O}(\epsilon)$ scalar mass. Graph 9-1 exists when we utilize the GMZ operator as our bare Lagrangian. Graph 9-2 exists when we utilize the non-local operator: the vertex depicted in this graph is the non-local vertex of Eq. (4.14). Graph 9-3 exists in either case, and gets its supersymmetry breaking from the gaugino mass.

(4.10)]. For these diagrams, as mentioned above, we are careful to keep a finite mass to deal with the infrared.

Summing the first six and either of the last two contributions from Table VI, we find below-threshold scalar mass dependence

$$\tilde{m}_\tau^2 \ni -2g_0'^4 Y_\tau^2 \sum_{\text{heavy}} Y_i^2 \frac{m_{3/2}^2}{(4\pi)^4 (\mu^2)^\epsilon (M^2)^\epsilon}. \quad (9.34)$$

This establishes Eq. (9.28), which is in turn equivalent to Eq. (9.26), making ultraviolet insensitivity explicit.

3. Finite computation for g'^4

Finally, a “completely finite” calculation, along the lines of that performed for the $(h^*h)^2$ case, is possible for the

TABLE IV. The one-loop $\mathcal{O}(\epsilon)$ contributions to the scalar mass. We have factored out the quantity $ig_0'^4 [1/(4\pi)^2] Y_\tau^2 m_{3/2}^2 (\mu^2)^{-\epsilon}$. Only one of Graph 9-1 or 9-2 contributes, depending on the form of the bare Lagrangian. The sum of Graph 9-1 and Graph 9-3 yields a total contribution which agrees with Eq. (9.27).

Graph 9-1	2ϵ
Graph 9-2	2ϵ
Graph 9-3	-4ϵ

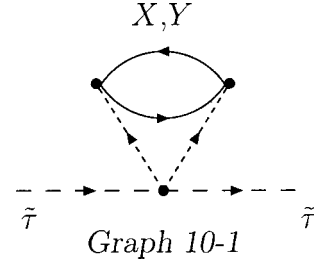


FIG. 10. ϵ -scalar diagram that contributes to the $g_0'^4$ contribution to the scalar mass. The supersymmetry breaking arises from the ϵ scalar mass.

gauge theory as well. Although at first glance it appears that the theory is unregulated, we can play the same game that we did in the Yukawa theory, and imagine that we are regulating the theory through the use of the Pauli-Villars regulators. After the X and Y Pauli-Villars regulator fields have been integrated out, a contribution proportional to $Y_X^2 Y_\tau^2$ arises, as shown in Eq. (9.25). Integrating out the physical X and Y particles should precisely cancel this anomaly-mediated contribution. This is the ultraviolet insensitivity. This calculation is outlined in Appendix B. The result of the finite calculation of Graphs 8-1 through 8-8 yields the following contribution: $[1/(4\pi)^4] 2m_{3/2}^2 g_0'^4 (\mu) Y_\tau^2 \sum_{\text{heavy}} Y_i^2$, which precisely cancels the corresponding term in Eq. (9.25).

X. CONCLUSION

We have discussed how DRED can be used for calculations in anomaly mediation. Including operators proportional to ϵ is absolutely essential, and failure to do so will yield incorrect results. For example, as we have shown, inclusion of the $\mathcal{O}(\epsilon)$ operators is vital for recovering ultraviolet insensitivity. We stress that inserting soft masses into the Lagrangian by hand and calculating with the resulting piecemeal Lagrangian will not give correct results. The failsafe procedure is to start with the bare Lagrangian given in Sec. IV and compute from there. The anomaly-mediated soft terms seamlessly emerge from these computations.

To demonstrate our DRED formalism, we have performed a diagrammatic calculation to shed light on the anomaly-mediated supersymmetry breaking scenario. In particular, we have shown explicitly how threshold corrections keep the supersymmetry-breaking parameters on anomaly-mediation trajectories. This result is not a surprise, considering the proof that already exists in the spurion calculus. However, it is interesting to see exactly how the great multiplicity of diagrams conspire to provide the necessary contributions and cancellations. Our calculation provides an explicit diagram-

TABLE V. Values to $\mathcal{O}(\epsilon^0)$ of the graphs contributing to the $g_0'^4$ correction to the scalar mass above threshold. We have omitted a common factor of $ig_0'^4 [1/(4\pi)^4] m_{3/2}^2 Y_\tau^2 \sum_{\text{heavy}} Y_i^2 (\mu^2)^{-2\epsilon}$.

Graph 8-6	6
Graph 8-6 Non-local	-2
Graph 10-1	-2

TABLE VI. Values to $O(\epsilon^0)$ of the graphs contributing to the $g_0'^4$ correction to the scalar mass below threshold. We have omitted a common factor of $ig_0'^4[1/(4\pi)^4]Y_7^2\Sigma_{\text{heavy}}Y_i^2m_{3/2}^2$. The integrals $I(m,n,l)$ are defined in Appendix A. The first set of entries correspond to diagrams where $\tilde{X}\tilde{Y}$ insertions have been made in the graphs. The multiple listings of Graph 8-6 represent the additional contributions that arise when one or both of the supersymmetry-breaking vertices of a $m_{3/2}M\tilde{X}\tilde{Y}$ mass insertion is replaced with supersymmetry-breaking gaugino mass vertex. The 8-6 (non-local) and 10-1 (GMZ) values enter alternately, depending on which Lagrangian is used. They are not to be added simultaneously toward the total contribution.

Graph 8-7 + 8-1	$\left(\frac{3}{\epsilon}-5-6\gamma\right)(M^2)^{-2\epsilon}$
Graph 8-1 (ϵ scalar)	$2(\mu^2)^{-\epsilon}(M^2)^{-\epsilon}$
Graph 8-3	$2I(3,1,1)-I(2,2,1)$ $=\left(\frac{1}{\epsilon}-1-2\gamma\right)(M^2)^{-2\epsilon}$
Graph 8-6	$\left(-\frac{4}{\epsilon}+2+8\gamma\right)(M^2)^{-2\epsilon}$
Graph 8-6 (One m_λ)	$-8(\mu^2)^{-\epsilon}(M^2)^{-\epsilon}+8(M^2)^{-2\epsilon}$
Graph 8-6 (Two m_λ)	$12(\mu^2)^{-\epsilon}(M^2)^{-\epsilon}-6(M^2)^{-2\epsilon}$
Graph 8-6 (Non-Local)	$-4(\mu^2)^{-\epsilon}(M^2)^{-\epsilon}+2(M^2)^{-2\epsilon}$
Graph 10-1 (GMZ)	$-4(\mu^2)^{-\epsilon}(M^2)^{-\epsilon}+2(M^2)^{-2\epsilon}$

matic check of the ultraviolet insensitivity.

Finally we mention that while the calculation in Sec. IX B refers to an Abelian model, it would be relatively straightforward to extend this discussion to a non-Abelian gauge theory.

ACKNOWLEDGMENTS

This was supported in part by the Director, Office of Science, Office of High Energy and Nuclear Physics, Division of High Energy Physics of the U.S. Department of Energy under Contract DE-AC03-76SF00098 and in part by the National Science Foundation under grant PHY-95-14797. A.P. are E.B. are also supported by the National Science Foundation. A.P. and H.M. would like to acknowledge helpful conversations with Zoltan Ligetti, Aneesh Manohar, and Stephen Martin. A.P. would like additionally to acknowledge discussions with David Smith and Yasunori Nomura.

APPENDIX A: EVALUATION OF THE INTEGRALS

Several diagrams contain similar integrals. In particular, it is useful to define

$$I(m,n,l)=\frac{1}{(2\pi)^8}\int\frac{d^4p}{(p^2-M^2)^m}\frac{d^4k}{(k^2-M^2)^n}\frac{1}{(k+p)^{2l}}, \quad (\text{A1})$$

and it is convenient to regularize the integrals using dimensional reduction.⁶

After performing the integrals, $I(m,n,l)$ can be expressed entirely in terms of beta functions (B). In particular,

$$I(m,n,l)=\frac{(-1)^{m+n+l+1}}{(4\pi)^{4-\epsilon}(M^2)^{n+m+l-4+\epsilon}}\frac{B(2,n+m-2)}{\Gamma(2-\epsilon)B(m,n)} \\ \times B(n+l-2+\epsilon,m+l-2+\epsilon) \\ \times B(2-l-\epsilon,n+m+l-4+\epsilon). \quad (\text{A2})$$

This expression can then be Taylor expanded to order ϵ , as shown in Table VII.

We also also define the following integrals which are useful in the evaluation of diagrams that include fermions:

$$F(m,n,l)\equiv\int\frac{k\cdot(p-k)}{(p^2)^l}\frac{d^4p}{((k-p)^2-M^2)^n} \\ \times\frac{d^4k}{(k^2-M^2)^m}, \quad (\text{A3})$$

and

$$G(m,n,l)\equiv\int\frac{k^2(k\cdot p)}{(p^2)^l}\frac{d^4p}{((k+p)^2-M^2)^n} \\ \times\frac{d^4k}{(k^2-M^2)^m}. \quad (\text{A4})$$

Using partial fraction decomposition, one can rewrite $F(m,n,l)$ and $G(m,n,l)$ in terms of $I(m,n,l)$. In particular, we find that

$$F(m,n,l)=\frac{-1}{2}[I(m-1,n,l)+I(m,n-1,l)+I(m,n,l-1)] \\ -M^2I(m,n,l), \quad (\text{A5})$$

and

$$G(m,n,l)=\frac{-1}{2}\{I(m-1,n-1,l)-I(m-2,n,l) \\ -I(m-1,n,l-1)+M^2[I(m,n-1,l) \\ -I(m-1,n,l)-I(m,n,l-1)]\}. \quad (\text{A6})$$

APPENDIX B: FINITE CALCULATIONS

Here we undertake the ‘‘finite’’ calculation of the h^4 correction in the Yukawa model and a similar calculation in the

⁶Both integrals must be continued to $4-2\epsilon$ dimensions, even though in practice one integral is completely finite in the mass insertion formalism. The reason is that the $\mathcal{O}(\epsilon)$ terms in the finite integral can combine with $1/\epsilon$ poles from the second integral to modify the finite pieces in the result.

TABLE VII. A list of series expansion useful in evaluation of $(h^*h)^2$ cancellations. We neglect the $\log(4\pi)$ and $\log(M^2)$ which cancel along with the Euler γ 's. There is also a common factor of $1/(4\pi)^4$.

Integral	Series expansion
$I(3,1,1)$	$\frac{1}{M^2} \left(\frac{1}{2\epsilon} - \frac{\gamma}{2} + \mathcal{O}(\epsilon) \right)$
$I(3,2,1)$	$\frac{1}{M^4} \left(-\frac{1}{4} + \mathcal{O}(\epsilon) \right)$
$I(3,3,1)$	$\frac{1}{M^6} \left(\frac{1}{12} + \mathcal{O}(\epsilon) \right)$
$I(4,1,1)$	$\frac{1}{M^4} \left(-\frac{1}{6\epsilon} - \frac{1}{12} + \frac{\gamma}{6} + \mathcal{O}(\epsilon) \right)$
$I(4,2,1)$	$\frac{1}{M^6} \left(\frac{1}{9} + \mathcal{O}(\epsilon) \right)$
$I(5,1,1)$	$\frac{1}{M^6} \left(\frac{1}{12\epsilon} + \frac{1}{18} - \frac{\gamma}{12} + \mathcal{O}(\epsilon) \right)$
$I(3,2,0)$	$\frac{1}{M^2} \left(\frac{1}{2\epsilon} - \frac{\gamma}{2} + \mathcal{O}(\epsilon) \right)$
$I(3,3,0)$	$\frac{1}{M^4} \left(-\frac{1}{4} + \mathcal{O}(\epsilon) \right)$
$I(4,1,0)$	$\frac{1}{M^2} \left(-\frac{1}{6\epsilon} - \frac{1}{6} + \frac{\gamma}{6} + \mathcal{O}(\epsilon) \right)$
$I(5,1,0)$	$\frac{1}{M^4} \left(\frac{1}{12\epsilon} + \frac{1}{12} - \frac{\gamma}{12} + \mathcal{O}(\epsilon) \right)$
$G(3,3,1)$	$\frac{1}{M^2} \left(\frac{-1}{\epsilon} + \frac{5}{4} + \gamma + \mathcal{O}(\epsilon) \right)$
$F(4,1,1)$	$\frac{1}{M^2} \left(\frac{2}{3\epsilon} + \frac{1}{3} - \frac{2\gamma}{3} + \mathcal{O}(\epsilon) \right)$
$F(5,1,1)$	$\frac{1}{M^4} \left(\frac{-1}{4\epsilon} - \frac{5}{24} + \frac{\gamma}{4} + \mathcal{O}(\epsilon) \right)$

gauge theory. First consider the Yukawa theory. Using Table II and Table VII, one can write the threshold correction (excluding the A -term contribution) as

$$\begin{aligned} \text{Sum of diagrams} &= i[h^*(\mu)h(\mu)]^2 (Mm_{3/2})^2 \\ &\times \left((4\pi)^{-4} \frac{-11}{6M^2} + 24M^4 I(5,1,1) \right. \\ &\left. + 30M^2 I(4,1,1) + 6I(3,1,1) \right). \quad (\text{B1}) \end{aligned}$$

Here, we have only used the expressions in Table VII for those integrals that are finite. Since we are not working in DRED here, there is no order ϵ contribution to these integrals.

Our remaining task is to calculate the combination $24M^4 I(5,1,1) + 30M^2 I(4,1,1) + 6I(3,1,1)$ without resorting to the regularization of any integrals. After a Wick rotation, we can write this combination as

$$\begin{aligned} &6 \int \frac{d^4 p d^4 k}{(2\pi)^8} \frac{1}{(k^2 + M^2)^3} \frac{1}{(k-p)^2 + M^2} \frac{1}{p^2} \\ &\times \left(1 - \frac{5M^2}{k^2 + M^2} + \frac{4M^4}{(k^2 + M^2)^2} \right). \quad (\text{B2}) \end{aligned}$$

This, in turn, can be written as

$$-6 \int \frac{d^4 p d^4 k}{(2\pi)^8} \frac{1}{(k-p)^2 + M^2} \frac{1}{p^2} \frac{1}{k^2} \frac{\partial}{\partial k^2} \frac{(k^2)^3}{(k^2 + M^2)^4}. \quad (\text{B3})$$

Now this integral can be done by first doing the k^2 integral by parts. The surface term vanishes, leaving

$$-3 \int \frac{d^4 p d^4 k}{(2\pi)^8} \frac{2k^4 - 2k^2(p \cdot k)}{[(k-p)^2 + M^2]^2} \frac{1}{(k^2 + M^2)^4}. \quad (\text{B4})$$

From this point, standard Feynman parameter techniques can be employed, yielding the result

$$24M^4 I(5,1,1) + 30M^2 I(4,1,1) + 6I(3,1,1) = (4\pi)^{-4} \frac{-7}{6M^2}. \quad (\text{B5})$$

Combining this with Eq. (B1) yields

$$\text{Sum of diagrams} = -3i[h^*(\mu)h(\mu)]^2 \frac{m_{3/2}^2}{(4\pi)^4}. \quad (\text{B6})$$

As discussed in the text, this combines with a contribution $+6i[h^*(\mu)h(\mu)]^2 [1/(4\pi)^4] m_{3/2}^2$ from the A -term diagram to yield the correct threshold correction for the scalar mass.

Incidentally, the calculation of the same integrals in dimensional regularization will yield $(-19/6M^2)(4\pi)^{-4}$. The difference results from the fact that the $d^4 k$ becomes a $d^{4-2\epsilon} k$ and the integration by parts picks up an extra piece.

Now consider the gauge theory. Again, the game will be to keep all integrals well defined without ever continuing to $4-2\epsilon$ dimensions. Since we stay in 4 dimensions, the evanescent operators do not arise, and we need only consider Graphs 8-1, 8-3, 8-6, and Graph 8-7. The key is combine these graphs first, avoiding any divergent (ill-defined) integrals.

Graph 8-3 can be written as

$$\begin{aligned} \text{Graph 8-3} &= m_{3/2}^2 M^2 g'^4(\mu) Y_\tau^2 \sum_{\text{heavy}} Y_i^2 \frac{1}{(4\pi)^2} \\ &\times \int \frac{d^4 p}{(2\pi)^4 p^2} \int \frac{z(2z-1) dz}{[M^2 - p^2 z(1-z)]^2}. \end{aligned} \quad (\text{B7})$$

By itself, this integral would be divergent at the end points of the Feynman parameter integral. So we must combine this expression with expressions for the remaining graphs before evaluation. Graph 8-6 can be written

$$\begin{aligned} \text{Graph 8-6} &= 4m_{3/2}^2 M^2 g'^4(\mu) Y_\tau^2 \sum_{\text{heavy}} Y_i^2 \frac{1}{(4\pi)^2} \\ &\times \int \frac{d^4 p}{(2\pi)^4 p^2} \int \frac{z^3 dz}{[M^2 - p^2 z(1-z)]^2}. \end{aligned} \quad (\text{B8})$$

Finally, we write the sum of Graphs 8-1 and 8-7 using the vacuum polarization operator:

$$\text{Graph 8-1} + \text{Graph 8-7} = -3ig'^2(\mu) \int \frac{\Pi(p^2) d^4 p}{(2\pi)^4 p^2}, \quad (\text{B9})$$

where $\Pi(p^2)$ is the vacuum polarization operator to $\mathcal{O}(m_{3/2}^2)$ in four dimensions. In the mass insertion formalism, it is given by the expression

$$\begin{aligned} \Pi(p^2) &\equiv \frac{im_{3/2}^2 M^2 (Y_{X_1}^2 + Y_{X_2}^2) g'^2(\mu)}{(4\pi)^2} \\ &\times \int \frac{(1-2z)^2 dz}{[M^2 - p^2 z(1-z)]^2}, \end{aligned} \quad (\text{B10})$$

which can be seen by taking the $\epsilon \rightarrow 0$ limit in Eq. (9.33).

Utilizing Eqs. (B7), (B8), (B9), and (B10), we can write the sum of diagrams as

$$\begin{aligned} \text{Graph 8-1} + \text{Graph 8-3} + \text{Graph 8-6} + \text{Graph 8-7} \\ &= -4i \frac{1}{(4\pi)^4} m_{3/2}^2 M^2 g'^4(\mu) Y_\tau^2 \sum_{\text{heavy}} Y_i^2 \\ &\times \int \int_0^1 \frac{z(1-z)^2 dz d^4 p}{p^2 [M^2 - p^2 z(1-z)]^2}. \end{aligned} \quad (\text{B11})$$

This integral is completely finite so no regulator is needed. The integral yields a contribution to the scalar mass

$$\begin{aligned} & - \frac{1}{i} (\text{Graph 8-1} + \text{Graph 8-3} + \text{Graph 8-6} + \text{Graph 8-7}) \\ &= \frac{1}{(4\pi)^4} 2m_{3/2}^2 M^2 g'^4(\mu) Y_\tau^2 \sum_{\text{heavy}} Y_i^2. \end{aligned} \quad (\text{B12})$$

This precisely corrects Eq. (9.25) to be Eq. (9.26), demonstrating the ultraviolet insensitivity.

APPENDIX C: CALCULATION OF WAVE-FUNCTION RENORMALIZATION IN GAUGE THEORY

To offer an alternative to direct computation, and to avoid the niceties of a supersymmetric (sans Wess-Zumino gauge) calculation of Z_τ , we can use renormalization group principles to determine \tilde{m}_τ^2 in terms of bare couplings. Working above threshold, the generic structure of two-loop diagrams tells us that Z_τ must be of the form

$$Z_\tau = 1 + A \frac{Y_\tau^2 g_0'^2}{(4\pi)^2 (\mu^2)^\epsilon} \frac{1}{\epsilon} + B \frac{Y_\tau^2 g_0'^4}{(4\pi)^4 (\mu^2)^{2\epsilon}} \frac{1}{\epsilon^2}. \quad (\text{C1})$$

Then

$$\begin{aligned} \gamma_\tau &\equiv -\frac{1}{2} \mu \frac{d}{d\mu} \log Z_\tau \\ &= A \frac{Y_\tau^2 g_0'^2}{(4\pi)^2 (\mu^2)^\epsilon} + 2B \frac{Y_\tau^2 g_0'^4}{(4\pi)^4 (\mu^2)^{2\epsilon}} \frac{1}{\epsilon} \\ &\quad - A^2 \frac{Y_\tau^4 g_0'^4}{(4\pi)^4 (\mu^2)^{2\epsilon}} \frac{1}{\epsilon}. \end{aligned} \quad (\text{C2})$$

The poles in γ_τ are lower order than the poles in Z_τ because μ derivatives hitting terms like $(\mu^2)^\epsilon$ bring down factors of ϵ .

We know that in the $\epsilon \rightarrow 0$ limit, the expression for γ_τ must agree with the expression in terms of the renormalized coupling to one-loop order. Comparing with Eq. (9.23) fixes $A = -2$, so that

$$\begin{aligned} \gamma_\tau &= -2 \frac{Y_\tau^2 g_0'^2}{(4\pi)^2 (\mu^2)^\epsilon} + 2B \frac{Y_\tau^2 g_0'^4}{(4\pi)^4 (\mu^2)^{2\epsilon}} \frac{1}{\epsilon} \\ &\quad - 4 \frac{Y_\tau^4 g_0'^4}{(4\pi)^4 (\mu^2)^{2\epsilon}} \frac{1}{\epsilon}. \end{aligned} \quad (\text{C3})$$

Now we work to fix B . We can do this by utilizing two pieces of information: the known expression for the running of the gauge coupling and the finiteness of γ_τ . To proceed we first write the bare coupling in terms of the renormalized coupling. They are equal at one loop, and at higher order we include an arbitrary parameter C to be completely general. We define the renormalized coupling as

$$g'^2(\mu) + Cg'^4(\mu) \equiv g_0'^2 - B \frac{g_0'^4}{(4\pi)^2(\mu^2)^\epsilon} \frac{1}{\epsilon} + 2 \frac{Y_\tau^2 g_0'^4}{(4\pi)^2(\mu^2)^\epsilon} \frac{1}{\epsilon}. \quad (\text{C4})$$

This form is convenient because it allows us to rewrite the γ_τ of Eq. (C3) simply in terms of renormalized couplings,

$$\gamma_\tau = -2 \frac{Y_\tau^2 g'^2(\mu)}{(4\pi)^2(\mu^2)^\epsilon} + C \frac{Y_\tau^2 g'^4(\mu)}{(4\pi)^4(\mu^2)^\epsilon}. \quad (\text{C5})$$

Now we make the critical observation that γ_τ is an observable quantity, and so it must be finite in the $\epsilon \rightarrow 0$ limit when expressed in terms of the renormalized coupling. In other words, C is finite. Now we can determine B by comparing our definition in Eq. (C4) with the known running of the gauge coupling constant:

$$g'^2(\mu) = g_0'^2 - \frac{g_0'^4 \left(Y_\tau^2 + \sum_{\text{heavy}} Y_i^2 \right)}{(4\pi)^2(\mu^2)^\epsilon} \frac{1}{\epsilon}. \quad (\text{C6})$$

Inserting this known expression for $g'^2(\mu)$ into Eq. (C4) and keeping up to $O(g'^4)$, we find the condition

$$g_0'^2 - \frac{g_0'^4 \left(Y_\tau^2 + \sum_{\text{heavy}} Y_i^2 \right)}{(4\pi)^2(\mu^2)^\epsilon} \frac{1}{\epsilon} + Cg_0'^4 = g_0'^2 - B \frac{g_0'^4}{(4\pi)^2(\mu^2)^\epsilon} \frac{1}{\epsilon} + 2 \frac{Y_\tau^2 g_0'^4}{(4\pi)^2(\mu^2)^\epsilon} \frac{1}{\epsilon}. \quad (\text{C7})$$

Equivalently,

$$B = \left(Y_\tau^2 + \sum_{\text{heavy}} Y_i^2 \right) + 2Y_\tau^2 - C\epsilon(4\pi)^2(\mu^2)^\epsilon. \quad (\text{C8})$$

But since C is finite and comes multiplied by ϵ , it makes at most a finite $O(g_0'^4)$ contribution to γ_τ , which is next-to-leading order in Eq. (C2). We have consistently been neglecting such terms. In short,

$$B = \left(Y_\tau^2 + \sum_{\text{heavy}} Y_i^2 \right) + 2Y_\tau^2. \quad (\text{C9})$$

We have determined that

$$\gamma_\tau = -2 \frac{Y_\tau^2 g_0'^2}{(4\pi)^2(\mu^2)^\epsilon} + 2 \frac{g_0'^4 Y_\tau^2 \left(Y_\tau^2 + \sum_{\text{heavy}} Y_i^2 \right)}{(4\pi)^4(\mu^2)^{2\epsilon}} \frac{1}{\epsilon}, \quad (\text{C10})$$

and differentiation yields the scalar mass in terms of bare couplings:

$$\tilde{m}_\tau^2 = \frac{m_{3/2}^2}{(4\pi)^2} \left(2 \frac{\epsilon Y_\tau^2 g_0'^2}{(\mu^2)^\epsilon} - 4 \frac{g_0'^4 Y_\tau^2 \left(Y_\tau^2 + \sum_{\text{heavy}} Y_i^2 \right)}{(4\pi)^2(\mu^2)^{2\epsilon}} \right) \quad (\text{above threshold, bare couplings}). \quad (\text{C11})$$

Below threshold, $\mu \ll M$, and the analysis is similar. In γ_τ we make the replacement $Y_i^2(\mu^2)^{-\epsilon} \rightarrow Y_i^2(M^2)^{-\epsilon}$ for the heavy particles, because their contributions to loop integrals are cut off at M . We then find

$$\gamma_\tau \rightarrow -2 \frac{Y_\tau^2 g_0'^2}{(4\pi)^2(\mu^2)^\epsilon} + 2 \frac{g_0'^4 Y_\tau^4}{(4\pi)^4(\mu^2)^{2\epsilon}} \frac{1}{\epsilon} + 2 \frac{g_0'^4 Y_\tau^2 \sum_{\text{heavy}} Y_i^2}{(4\pi)^4(\mu^2)^\epsilon (M^2)^\epsilon} \frac{1}{\epsilon}. \quad (\text{C12})$$

Clearly then

$$\tilde{m}_\tau^2 = \frac{m_{3/2}^2}{(4\pi)^2} \left(2 \frac{\epsilon Y_\tau^2 g_0'^2}{(\mu^2)^\epsilon} - 4 \frac{g_0'^4 Y_\tau^4}{(4\pi)^2(\mu^2)^{2\epsilon}} - 2 \frac{g_0'^4 Y_\tau^2 \sum_{\text{heavy}} Y_i^2}{(4\pi)^2(\mu^2)^\epsilon (M^2)^\epsilon} \right) \quad (\text{below threshold, bare couplings}). \quad (\text{C13})$$

-
- [1] R. Sundrum and L. Randall, Nucl. Phys. **B557**, 79 (1999).
[2] G.F. Giudice, M. Luty, H. Murayama, and R. Rattazzi, J. High Energy Phys. **12**, 027 (1998).
[3] A. Pomarol and R. Rattazzi, J. High Energy Phys. **05**, 013 (1999).
[4] E. Katz, Y. Shadmi, and Y. Shirman, J. High Energy Phys. **08**, 015 (1999).
[5] N. Arkani-Hamed, D.E. Kaplan, H. Murayama, and Y. No-

- mura, J. High Energy Phys. **02**, 041 (2001); I. Jack and D.R.T. Jones, Phys. Lett. B **482**, 167 (2000).
[6] W. Seigel, Phys. Lett. **84B**, 193 (1979).
[7] I. Jack and D.R. Jones, Phys. Lett. B **465**, 148 (1999).
[8] M. A. Luty and R. Sundrum, Phys. Rev. D **65**, 066004 (2002).
[9] N. Arkani-Hamed and H. Murayama, J. High Energy Phys. **06**, 030 (2000).
[10] V. Kaplunovsky and J. Louis, Nucl. Phys. **B422**, 57 (1994).

- [11] N. Arkani-Hamed, G.F. Giudice, M.A. Luty, and R. Rattazzi, Phys. Rev. D **58**, 115005 (1998).
- [12] G.F. Giudice and R. Rattazzi, Nucl. Phys. **B511**, 25 (1998).
- [13] J. Hisano and M. Shifman, Phys. Rev. D **56**, 5475 (1997).
- [14] M.T. Grisaru, B. Milewski, and D. Zanon, Phys. Lett. **155B**, 357 (1985).
- [15] I. Jack, D.R. Jones, S.P. Martin, M.T. Vaughn, and Y. Yamada, Phys. Rev. D **50**, 5481 (1994).
- [16] S. Martin, Phys. Rev. D **55**, 3177 (1997); S. Dimopoulos, G.F. Giudice, and A. Pomarol, Phys. Lett. B **389**, 37 (1996).